of St2b2 and INV. St2b2 protein levels decreased to 60% of those in control skin following infection with AdSt2b2-shRNA (Fig. 6A). St2b2 proteins level increased by 30% after TPA treatment in control skin, but were not significantly affected by TPA treatment in AdSt2b2-shRNA–infected skin (Fig. 6A). Ch-ST activity also increased by 50% after TPA treatment in control skin, but not in AdSt2b2-shRNA–infected skin (Fig. 6B). INV protein levels increased by 40% after TPA treatment in control skin, but not in AdSt2b2-shRNA–infected skin (Fig. 6C).

Time-Dependent Changes in St2b2, INV, and TNFα Expression after TPA Treatment in NME Cells To explore the potential involvement of TNFα in TPA-induced enhancement of St2b2 and INV expression, time-dependent changes in the expression profiles of these proteins were examined after TPA treatment in NME cells. Significant increases in St2b2 expression were observed after 24 h (Fig. 7A). INV expression also increased after 24 h (Fig. 7B). Cellular levels of TNFα protein peaked within 3 h of TPA treatment (Fig. 7C), whereas extracellular levels reached a maximum at 24 h (Fig. 7D).

Effects of TNFα on St2b2 and INV Expression in NME Cells To examine the role of TNFα in TPA-induced enhancement of St2b2 expression, NME cells were treated with TNFα. St2b2 protein levels increased by up to 260% after TNFα treatment (Fig. 8A). INV protein levels also similarly increased (by a maximum of 210%; Fig. 8B). Maximum effects for both proteins were observed with 30 pg/ml TNFα.

Effects of Knocking Down St2b2 Expression on TNFα-Induced INV Expression in NME Cells AdSt2b2-shRNA was then used to examine the roles of St2b2 on enhanced INV expression in NME cells. St2b2 protein expression levels in TNFα-treated cells decreased from 410 to 130% of those observed in control cells after AdSt2b2-shRNA infection (Fig. 9A). AdSt2b2-shRNA infection also decreased INV protein expression in TNFα-treated cells from 330 to 130% of control levels (Fig. 9B).

Effects of Inhibiting TNFα Signaling on TPA-Induced Enhancement of St2b2 and INV Expression in NME Cells To verify that TNFα signaling mediates the TPA-induced enhancement of St2b2 and INV expression, TNFα-siRNA was introduced into NME cells. TNFα protein levels in the

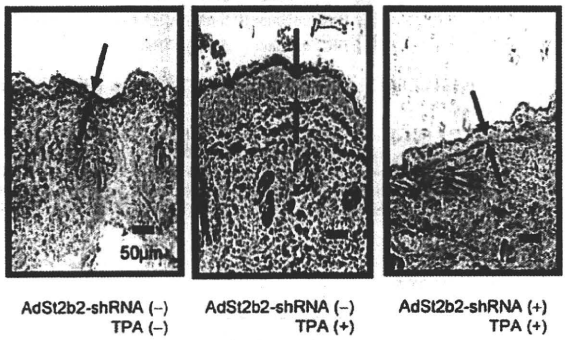

Fig. 5. Effects of AdSt2b2-shRNA on TPA-Induced Hyperplasia in Mouse Epidermis

Shaved skin was painted with a suspension containing 1.0×10^7 $TCID_{50}$ of AdSt2b2-shRNA or AdControl, and the mice were treated with TPA (16 nmol) or acetone (vehicle) 24 h after adenovirus infection. The skin was removed 40 h after TPA treatment. The thickness of the epidermis was determined using frozen sections stained with methyl green-pyronin. The epidermis is shown between the arrows. Scale bars represent 50 μm.

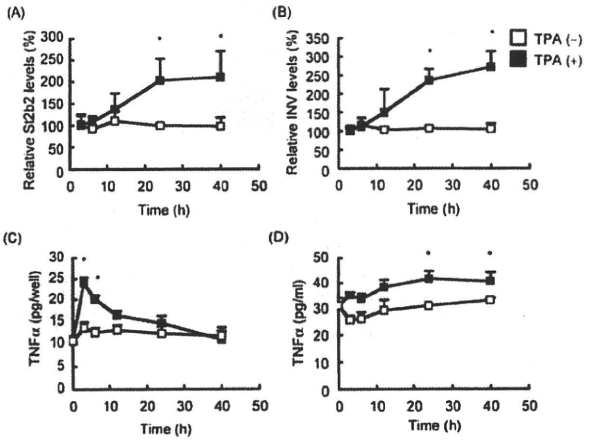

Fig. 7. Expression of TNFα, St2b2, and INV after TPA Treatment in NME Cells

NME cells (3×10^4 cells/cm^2) were cultured in medium containing 10 nM TPA or 0.1% (v/v) DMSO (vehicle), and harvested 0, 3, 6, 12, 24, or 40 h after TPA treatment. Levels of St2b2 protein in the cytosol (A) and INV protein in the membrane fraction (B) were determined by immunoblotting. The levels are shown as ratios to those detected at 3 h. TNFα levels in the S-9 fraction (C) and the medium (D) were determined using ELISAs. Data are shown as means±S.D. (n=3). *p<0.05 (St2b2 and INV, *vs.* vehicle-treated TPA(−) cells at 3 h; TNFα, *vs.* vehicle-treated TPA(−) cells at 0 h).

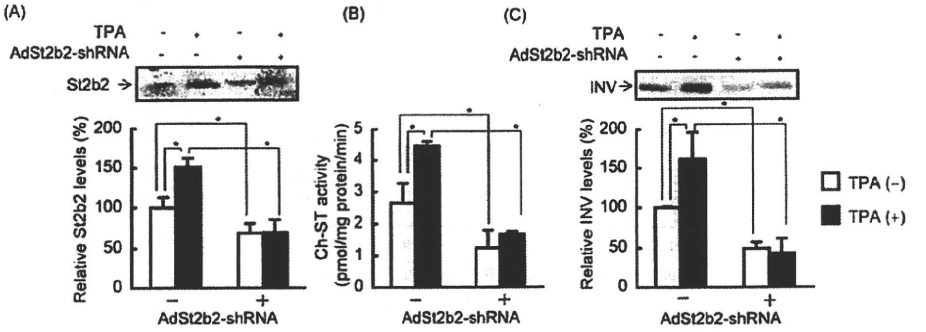

Fig. 6. Effects of Knocking Down St2b2 Gene Expression on TPA-Induced Epidermal Differentiation

Mice were treated with AdSt2b2-shRNA and TPA as described in the legend for Fig. 5. Levels of St2b2 protein in the cytosol (A) and INV protein in the membrane fraction (B) were determined by immunoblotting. Membranes immunoblotted for St2b2 and INV are shown above the graphs. The expression levels are shown as ratios to those in control AdSt2b2-shRNA(−) and TPA(−) epidermis. Ch-ST activity in the cytosol (C) was also assessed. Data are shown as means±S.D. (n=3). *p<0.05.

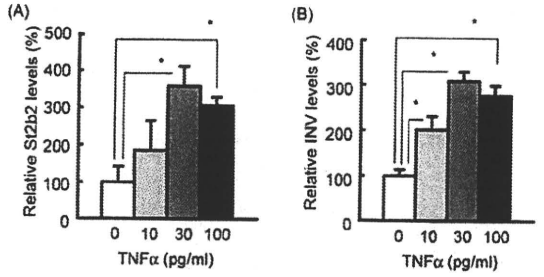

Fig. 8. Effects of TNFα Treatment on St2b2 and INV Expression in NME Cells

NME cells (3×10^5 cells/cm^2) were cultivated in medium containing TNFα (10, 30, or 100 pg/ml) or 2 μg/ml BSA-PBS (vehicle) for 24 h. Levels of St2b2 protein in the cytosol (A) and INV protein in the membrane fraction (B) were determined by immunoblotting. The expression levels are shown as ratios to those in control cells. Data are shown as means±S.D. (n=3). * p<0.05 *vs.* vehicle-treated TNFα(−) cells.

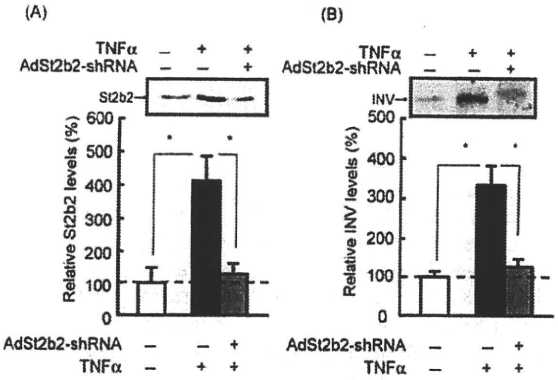

Fig. 9. Effects of Knocking Down St2b2 Expression on TNFα-Induced Enhancement of St2b2 and INV Expression in NME Cells

NME cells (3×10^5 cells/cm^2) were infected with AdSt2b2-shRNA (MOI: 6), and, 24 h later, the cells were treated with 30 pg/ml TNFα or 2 μg/ml BSA-PBS (vehicle) for 24 h. Levels of St2b2 protein in the cytosol (A) and INV protein in the membrane fraction (B) were determined by immunoblotting. Membranes immunoblotted for St2b2 and INV are shown above the graphs. Expression levels are shown as ratios to those in control AdSt2b2-shRNA(−) and TNFα(−) cells. Data are shown as means±S.D. (n=3). * p<0.05.

medium increased to 45 pg/ml after TPA treatment (control cells produced 21 pg/ml). On the other hand, TNFα protein levels did not increase after TPA treatment in the presence of TNFα-siRNA; TPA-treated cells that were also exposed to 90 nM TNFα-siRNA produced 22 pg/ml TNFα (Fig. 10A). St2b2 protein levels in TPA-treated cells (190% of levels detected in control cells) decreased to 100% of those observed in control cells after treatment with 90 nM TNFα-siRNA (Fig. 10B). TPA-induced enhancement of INV expression (150% of levels in control cells) also decreased to 100% of that in control cells after treatment (Fig. 10C).

To confirm further the involvement of TNFα in TPA-induced enhancement of St2b2 and INV expression, St2b2 and INV protein levels were examined in NME cells treated with TNFR-Ab and TPA. TNF-Ab (8 μg/ml) reduced TPA-induced enhancement of St2b2 expression (170% of that in control TNFR-Ab(−) and TPA(−) cells) to 70% of that observed in the control cells (Fig. 11A). The TPA-induced enhancement of INV expression (160% of that in control cells) was also reduced to 110% of that detected in control cells after treatment (Fig. 11B). No marked difference was observed in extracellular TNFα protein levels before and after treatment (data not shown).

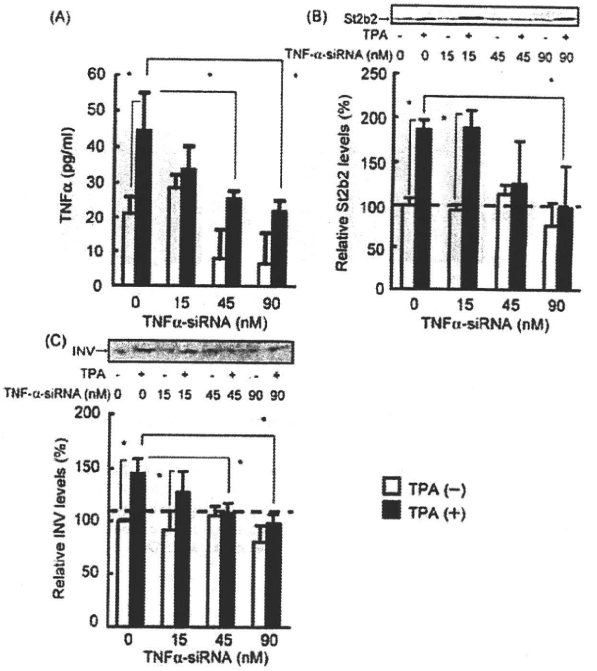

Fig. 10. Effects of Knocking Down TNFα Expression on TPA-Induced Enhancement of St2b2 and INV Expression in NME Cells

NME cells (3×10^5 cells/cm^2) were transfected with TNFα-siRNA (15, 45, or 90 nM). The total amount of siRNA was adjusted to 90 nM using Control-siRNA A. Twenty-four hours later, the cells were treated with 10 nM TPA or 0.1% (v/v) DMSO (vehicle) for 40 h. (A) TNFα protein levels in the medium were determined using an ELISA. Levels of St2b2 protein in the cytosol (B) and INV protein in the membrane fraction (C) were determined by immunoblotting. Expression levels are shown as ratios to those in control TNFα-siRNA(−) and TPA(−) cells. Data are shown as means±S.D. (n=3). * p<0.05.

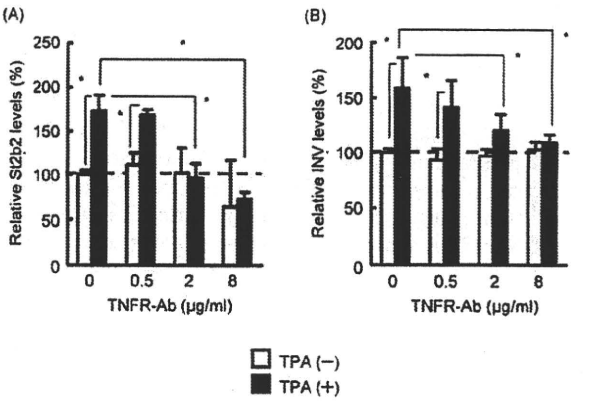

Fig. 11. Effects of TNFR Inhibition on TPA-Induced Enhancement of St2b2 and INV Expression in NME Cells

NME cells (3×10^5 cells/cm^2) were incubated with 0.5, 2, or 8 μg/ml TNFR-Ab for 6 h. The total amount of antibody was adjusted to 8 μg/ml with normal IgG. The cells were then cultivated in medium containing 10 nM TPA or 0.1% (v/v) DMSO (vehicle) for 40 h. St2b2 protein levels in the cytosol (A) and INV protein levels in the membrane fraction (B) were determined by immunoblotting. Expression levels are shown as ratios to those in control TNFR-Ab(−) and TPA(−) cells. Data are shown as means±S.D. (n=3). * p<0.05.

Effects of NF-κB Inhibition on TNFα-Induced Enhancement of St2b2 and INV Expression in NME Cells

NF-κB, which is activated through TNFα–TNFR signaling,

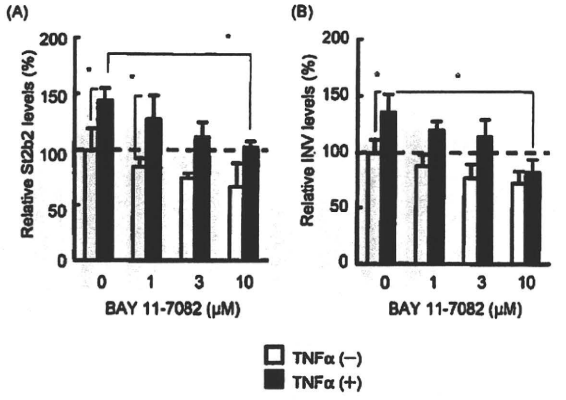

Fig. 12. Effects of NF-κB Inhibition on TNFα-Induced Enhancement of St2b2 and INV Expression in NME Cells

NME cells (3×10^5 cells/cm^2) were incubated with BAY 11-7082 (1, 3, or 10 μM) for 1 h, and then cultivated with 30 pg/ml TNFα or 2 μg/ml BSA-PBS (vehicle) for 24 h. Levels of St2b2 protein in the cytosol (A) and INV protein in the membrane fraction (B) were determined by immunoblotting. Expression levels are shown as ratios to those in the control BAY 11-7082(−) and TNFα(−) cells. Data are shown as the means±S.D. ($n=3$). *$p<0.05$.

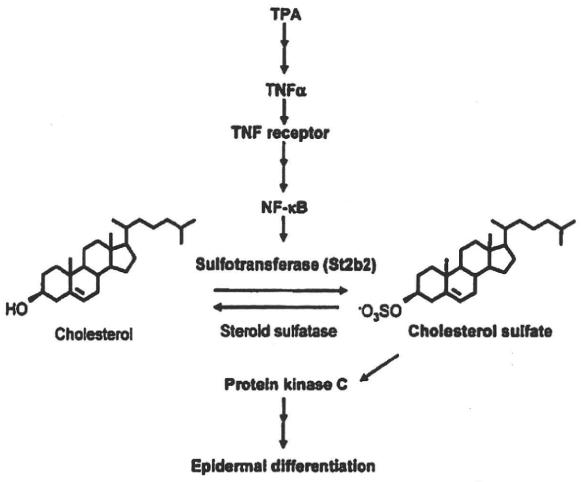

Fig. 13. A Putative Pathway for TPA-Induced Epidermal Differentiation through St2b2

plays a critical role in cell differentiation.[25] To examine NF-κB during TPA-induced enhancement of St2b2 and INV expression, an NF-κB inhibitor, BAY 11-7082, was administered to NME cells. BAY 11-7082 (10 μM) decreased TNFα-induced enhancement of St2b2 expression (140% of that in control BAY 11-7082(−) and TNFα(−) cells) to 100% of that in control cells (Fig. 12A). TNFα-induced enhancement of INV expression (140% of levels observed in control cells) decreased to 80% of levels in control cells after treatment (Fig. 12B).

DISCUSSION

CS is involved in epidermal differentiation and, at high concentrations, causes epidermal hyperplasia. Skin CS levels are believed to be maintained by both Ch-ST and SSase. In the present study, TPA-mediated CS accumulation in the epidermis occurred in parallel with increased Ch-ST activity, without changes in SSase activity (Table 2). Expression of St2b2 mRNA and protein in mouse skin increased after TPA treatment (Fig. 2). These results were consistent with the idea that TPA-mediated CS production mainly results from enhanced St2b2 expression.

To assess St2b2 functions during TPA-induced epidermal hyperplasia and differentiation, St2b2 gene expression was knocked down using shRNA in mice. TPA-induced epidermal hyperplasia was clearly blocked by St2b2-shRNA (Fig. 5). Decreases in INV and St2b2 expression were also observed in epidermis tissue infected with AdSt2b2-shRNA (Fig. 6). These results suggested that an increase in St2b2 levels is a prerequisite for TPA-induced epidermal hyperplasia.

PKC activation is involved in the differentiation of many cell lines, including epidermal cells, and is a key process during TPA-induced epidermal differentiation.[26–28] TPA was reported to activate PKC *via* direct binding[29]; this study suggested that direct binding triggers TPA-induced epidermal differentiation, but the mechanism for PKC activation during TPA-induced epidermal differentiation has not been elucidated. In the present study, TPA-induced epidermal differentiation and hyperplasia were suppressed by inhibition of increases in St2b2 expression, the primary cause of increased CS concentrations after TPA treatment (Figs. 5, 6). CS may be involved in epidermal differentiation through the activation of PKC.[13,30] Combined with our present results obtained with a PKC inhibitor (Fig. 4), TPA-induced PKC activation appears to result from increased St2b2 expression and consequent elevations in CS concentrations.

Our results suggest that TPA-induced increases in CS concentrations cause hyperplasia (Figs. 3, 5, 6). TPA stimulates proliferation and differentiation in skin epidermis *via* activation of several forms of PKC. Knocking down St2b2 expression, and consequent inhibition of CS biosynthesis, likely inhibited epidermal differentiation and blocked hyperplasia. Previous reports showed that successive doses of CS inhibited the tumor-promoting effects of TPA in mouse skin.[30] Chida *et al.* also reported that a single large dose of CS (400 μg) caused desquamation but not proliferation. Together, these results suggest that repeated high doses of CS inhibit TPA-induced tumorigenesis.

The anti-inflammatory agent indomethacin decreased TPA-mediated increases in Ch-ST activity and epidermal hyperplasia.[22,31] This suggested that inflammatory cytokines mediate the enhanced St2b2 expression after TPA treatment. In fact, TNFα did not promote INV expression in the absence of increased St2b2 expression (Fig. 9). In addition, TPA-induced St2b2 expression diminished when TNFα signaling was suppressed (Fig. 10). Inhibiting TNFα binding to TNFR also reduced St2b2 expression (Fig. 11). These results indicated that TNFα triggers St2b2 expression in TPA-induced epidermal hyperplasia and differentiation.

NF-κB is known to participate in TPA-induced epidermal hyperplasia.[32–34] In the present study, an NF-κB inhibitor suppressed TNFα-induced expression of cornified envelope proteins and St2b2 (Fig. 12). These results suggest that TNFα–NF-κB signaling regulates St2b2 expression during TPA-induced epidermal hyperplasia. In fact, a putative NF-κB binding sequence was found in the 5′-flanking region of

the St2b2 gene (DNASIS software version 3.0, Hitachi Software Engineering Co., Tokyo, Japan). Therefore, St2b2 expression may increase owing to NF-κB activation of gene transcription. We also identified putative NF-κB binding sequences in the 5′-flanking region of the human Ch-ST ST2B1. In addition, ST2B1 expression increased when the LS174T human epithelial colon carcinoma cell line was treated with TPA or TNFα (unpublished results, Matsuda *et al.*). Thus, NF-κB may be involved in TPA-induced enhancement of ST2B expression in humans as well.

TNFα-siRNA decreased TNFα levels in the medium but not the expression of St2b2 or INV protein in the group not treated with TPA (Fig. 10). Neither TNFR-Ab nor BAY 11-7082 significantly inhibited basal expression levels of St2b2 and INV (Figs. 11, 12). These results suggested that TNFα–NF-κB signaling does not drive constitutive expression of St2b2 and INV, although the mechanisms underlying basal expression of these proteins remain unknown.

In conclusion, St2b2 is required for TPA-induced epidermal hyperplasia, a relationship that involves TNFα–NF-κB signaling. Our hypothesis for the mechanism of TPA-induced epidermal differentiation is shown in Fig. 13. TPA increases TNFα levels to activate NF-κB following binding to TNFR. Then, NF-κB activates St2b2 gene transcription, leading to an increase in the levels of St2b2 and epidermal CS. Finally, increased epidermal CS concentrations enhance the expression of cornified envelope proteins, such as INV, through PKC activation.

Acknowledgements We thank Mr. Hiroyuki Takatoku for technical support.

REFERENCES

1) Ekanayake-Mudiyanselage S., Aschauer H., Schmook F. P., Jensen J. M., Meingassner J. G., Proksch E., *J. Invest. Dermatol.*, **111**, 517—523 (1998).
2) Greenberg C. S., Birckbichler P. J., Rice R. H., *FASEB J.*, **5**, 3071—3077 (1991).
3) Takigawa M., Verma A. K., Simsiman R. C., Boutwell R. K., *Biochem. Biophys. Res. Commun.*, **105**, 969—976 (1982).
4) Castagna M., Takai Y., Kaibuchi K., Sano K., Kikkawa U., Nishizuka Y., *J. Biol. Chem.*, **257**, 7847—7851 (1982).
5) Kikkawa U., Takai Y., Tanaka Y., Miyake R., Nishizuka Y., *J. Biol. Chem.*, **258**, 11442—11445 (1983).
6) Nakadate T., *Jpn. J. Pharmacol.*, **49**, 1—9 (1989).
7) Elias P. M., Williams M. L., Maloney M. E., Bonifas J. A., Brown B. E., Grayson S., Epstein E. H. Jr., *J. Clin. Invest.*, **74**, 1414—1421 (1984).
8) Koppe G., Marinkovic-Ilsen A., Rijken Y., De Groot W. P., Jobsis A. C., *Arch. Dis. Child.*, **53**, 803—806 (1978).
9) Zettersten E., Man M. Q., Sato J., Denda M., Farrell A., Ghadially R., Williams M. L., Feingold K. R., Elias P. M., *J. Invest. Dermatol.*, **111**, 784—790 (1998).
10) Shimada M., Kamiyama Y., Sato A., Honma W., Nagata K., Yamazoe Y., *J. Biochem.*, **131**, 167—169 (2002).
11) Shimada M., Matsuda T., Sato A., Akase T., Matsubara T., Nagata K., Yamazoe Y., *Xenobiotica*, **38**, 1487—1499 (2008).
12) Jetten A. M., George M. A., Pettit G. R., Herald C. L., Rearick J. I., *J. Invest. Dermatol.*, **93**, 108—115 (1989).
13) Kiguchi K., Kagehara M., Higo R., Iwamori M., DiGiovanni J., *J. Invest. Dermatol.*, **111**, 973—981 (1998).
14) Djian P., Phillips M., Easley K., Huang E., Simon M., Rice R. H., Green H., *Mol. Biol. Evol.*, **10**, 1136—1149 (1993).
15) Eckert R. L., Yaffe M. B., Crish J. F., Murthy S., Rorke E. A., Welter J. F., *J. Invest. Dermatol.*, **100**, 613—617 (1993).
16) Crish J. F., Howard J. M., Zaim T. M., Murthy S., Eckert R. L., *Differentiation*, **53**, 191—200 (1993).
17) Watt F. M., *J. Invest. Dermatol.*, **81**, 100s—103s (1983).
18) Kohler H. B., Huchzermeyer B., Martin M., De Bruin A., Meier B., Nolte I., *Vet. Dermatol.*, **12**, 129—137 (2001).
19) Sen C. K., Packer L., *FASEB J.*, **10**, 709—720 (1996).
20) Murakawa M., Yamaoka K., Tanaka Y., Fukuda Y., *Biochem. Pharmacol.*, **71**, 1331—1336 (2006).
21) Scott K. A., Moore R. J., Arnott C. H., East N., Thompson R. G., Scallon B. J., Shealy D. J., Balkwill F. R., *Mol. Cancer Ther.*, **2**, 445—451 (2003).
22) Yamamoto S., Jiang H., Kato R., *Carcinogenesis*, **12**, 1145—1147 (1991).
23) Bradford M. M., *Anal. Biochem.*, **72**, 248—254 (1976).
24) Xu X. X., Lambeth J. D., *J. Biol. Chem.*, **264**, 7222—7227 (1989).
25) Chen G., Goeddel D. V., *Science*, **296**, 1634—1635 (2002).
26) Dlugosz A. A., Mischak H., Mushinski J. F., Yuspa S. H., *Mol. Carcinog.*, **5**, 286—292 (1992).
27) Ohba M., Ishino K., Kashiwagi M., Kawabe S., Chida K., Huh N. H., Kuroki T., *Mol. Cell. Biol.*, **18**, 5199—5207 (1998).
28) Osada S., Mizuno K., Saido T. C., Akita Y., Suzuki K., Kuroki T., Ohno S., *J. Biol. Chem.*, **265**, 22434—22440 (1990).
29) Zhang G., Kazanietz M. G., Blumberg P. M., Hurley J. H., *Cell*, **81**, 917—924 (1995).
30) Chida K., Murakami A., Tagawa T., Ikuta T., Kuroki T., *Cancer Res.*, **55**, 4865—4869 (1995).
31) Fischer S. M., Gleason G. L., Mills G. D., Slaga T. J., *Cancer Lett.*, **10**, 343—350 (1980).
32) Amigo M., Paya M., Braza-Boils A., De Rosa S., Terencio M. C., *Life Sci.*, **82**, 256—264 (2008).
33) Lizzul P. F., Aphale A., Malaviya R., Sun Y., Masud S., Dombrovskiy V., Gottlieb A. B., *J. Invest. Dermatol.*, **124**, 1275—1283 (2005).
34) Seitz C. S., Lin Q., Deng H., Khavari P. A., *Proc. Natl. Acad. Sci. U.S.A.*, **95**, 2307—2312 (1998).

Molecular Genetics and Metabolism 102 (2011) 91–98

Contents lists available at ScienceDirect

Molecular Genetics and Metabolism

journal homepage: www.elsevier.com/locate/ymgme

Functional analysis of genetic variations in the 5′-flanking region of the human MDR1 gene

Mayumi Saeki, Kouichi Kurose, Ryuichi Hasegawa, Masahiro Tohkin *

Division of Medicinal Safety Science, National Institute of Health Sciences, 1-18-1 Kamiyoga, Setagaya-ku, Tokyo 158-8501, Japan

ARTICLE INFO

Article history:
Received 26 August 2010
Accepted 26 August 2010
Available online 19 September 2010

Keywords:
5′-flanking region
Multidrug resistance 1
Nuclear receptors
P-glycoprotein
Single nucleotide polymorphism

ABSTRACT

P-glycoprotein (P-gp), the product of the *MDR1* gene, shows large interindividual variations in expression, which leads to differences in the pharmacokinetics of the substrate drugs. The functions of single nucleotide polymorphisms located in the nuclear receptor-responsive element of the 5′-flanking region in the human *MDR1* gene were analyzed in order to clarify the mechanism underlying the interindividual variation in P-gp expression. Electrophoretic mobility shift assays revealed that the −7833C>T substitution in the nuclear receptor-responsive region of *MDR1* decreases the binding affinities of four nuclear receptors to their responsive elements: vitamin D receptor (VDR), thyroid hormone receptor (TR), constitutive androstane receptor (CAR), and pregnane X receptor (PXR). A reporter gene assay revealed that the C-to-T substitution at −7833 also reduces the transcriptional activation of *MDR1* by VDR, TRβ, CAR, and PXR. However, another SNP (−1211T>C substitution), which results in the formation of a xenobiotic responsive element-like sequence and a hypoxia responsive element-like sequence, failed to affect the aryl hydrocarbon receptor-dependent and hypoxia-induced transcriptional activation of *MDR1*. Although the frequency of the −7833C>T substitution in *MDR1* is relatively low, the SNP is crucial because it may alter the pharmacokinetics of P-gp substrates in a small subset of the population.

1. Introduction

P-glycoprotein (P-gp) transports a wide variety of compounds, including foreign xenobiotics and endogenous substrates, to the outside of cells [1,2]. P-gp is encoded by the human *MDR1* gene and is expressed in various physiological barriers such as intestinal epithelium [3,4], kidney tubules cells [3], the liver [3], and the capillary endothelium of the central nervous system [5]. It also plays an important role in pharmacokinetic processes such as drug absorption [1,6–8], renal secretion [9], biliary excretion [10], and brain distribution [11–13]. The large interindividual variations in P-gp expression and activity levels [14–17] suggest that the systemic exposure level and tissue concentrations of drugs that are P-gp substrates vary depending on the subject [15,18]. The pharmacokinetic differences ultimately lead to interindividual variation in drug efficacy and adverse reactions. Therefore, P-gp expression levels and activity are crucial factors in drug efficacy and safety.

The results of several studies suggest that the basis of interindividual variation in P-gp expression and activity resides in the presence of single nucleotide polymorphisms (SNPs) in the coding region of *MDR1* [2,19–22]. Hoffmeyer et al. showed that 3435C>T, a synonymous SNP in exon 26, is associated with reduced P-gp expression in the duodenum and increased plasma levels of digoxin, a typical P-gp substrate, following its oral administration to healthy volunteers [23].Wang et al. also reported that 3435C>T appears to affect the allelic variation of MDR1 expression in the liver via a change in mRNA stability [24]. In addition to digoxin, other studies have reported that the T allele of 3435C>T is related to higher plasma concentrations of cyclosporine A. While these reports suggest the importance of *MDR1* exonic SNPs in the regulation of P-gp expression, conflicting results have been reported [18,23,25–27].

In addition to SNPs in the coding region, there are variations in the 5′-flanking region that could affect *MDR1* gene transcription and mRNA expression levels. Haplotypes in the *MDR1* transcriptional regulatory region suggest the existence of functional haplotypes that could alter P-gp expression [17,28,29]. In these studies, the −1789G>A haplotype, alone or in combination with −145C>G, was associated with decreased P-gp expression. However, the reported effects on P-gp expression of haplotypes carrying −129T>C and two other linked SNPs were contradictory, showing reduction and enhancement [27,30,31]. These reports suggest that functional SNPs in the 5′-flanking region have not been fixed, and the relationship between these SNPs and the transcriptional factors that regulate the *MDR1* gene transcription is unknown. Therefore, the mechanism underlying interindividual variations in the expression levels of P-gp remains unclear.

Geick et al. found that the induction of MDR1 mRNA by rifampicin is mediated by pregnane X receptor (PXR), which binds to direct

* Corresponding author. Fax: +81 3 3700 9788.
E-mail address: tohkin@nihs.go.jp (M. Tohkin).

1096-7192/$ – see front matter © 2010 Elsevier Inc. All rights reserved.
doi:10.1016/j.ymgme.2010.08.019

repeat sequences separated by four bases (DR4) located −7.9 to −7.8 kbp upstream of the transcription start site [32]. This region contains several DR sequences and functions as the enhancer region in *MDR1* [32]. The constitutive androstane receptor (CAR) also induces MDR1 mRNA expression by binding to several DR4s located in the same region [33]. Recently, we reported that the thyroid hormone receptor β (TRβ) and vitamin D receptor (VDR) regulate the expression of *MDR1* by binding to several DRs located in this region [34,35]. A SNP, −7833C>T, has been reported within one of the half-sites (Hs), a pair of which composes a DR or ER (AGTTCA>AGTTTA,

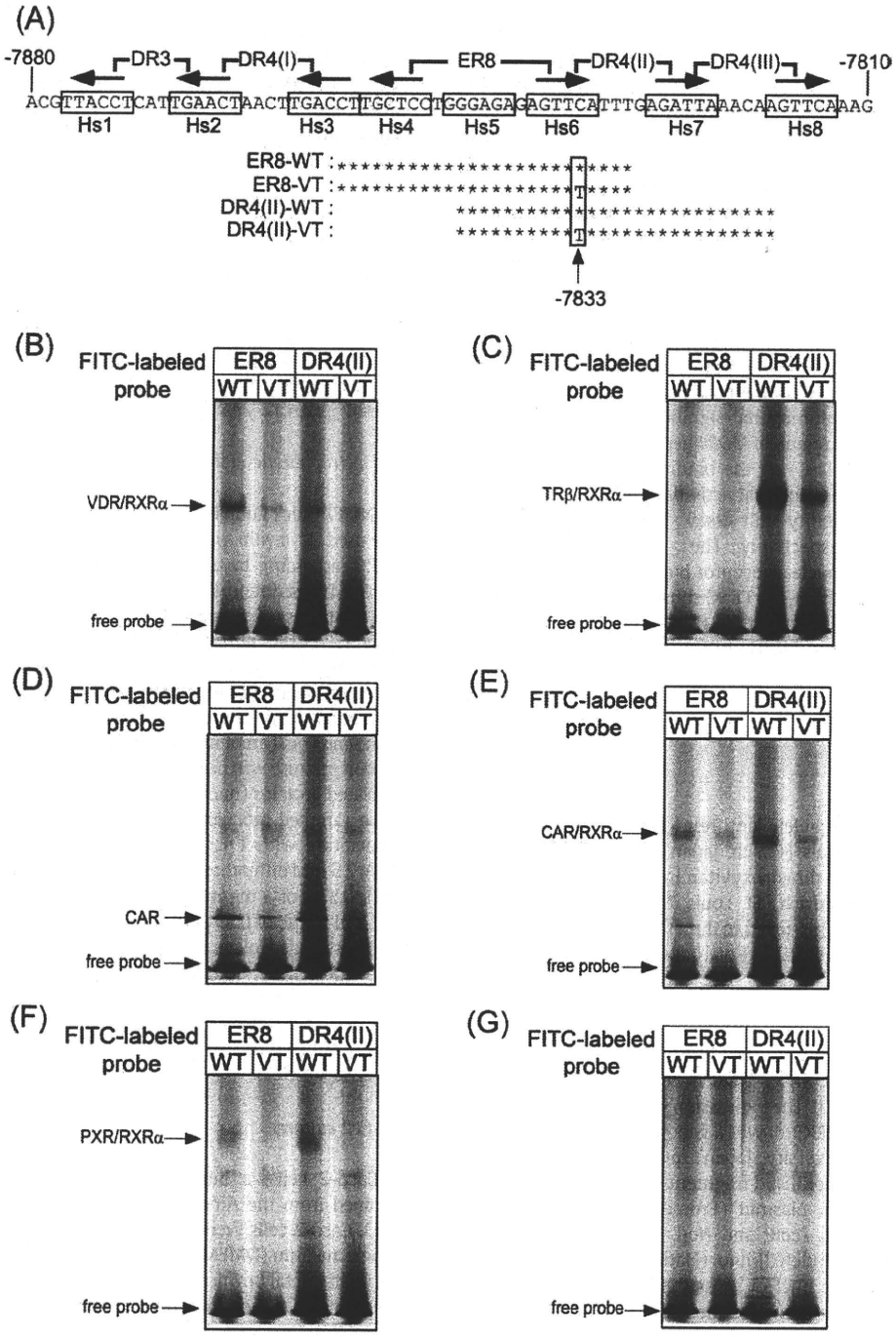

Fig. 1. The C-to-T substitution at −7833 affects the binding affinity of nuclear receptors to ER8 and/or DR4(II) in the *MDR1* gene. (A) Oligonucleotide sequences used for the electrophoretic mobility shift assay (EMSA). Several half-sites (designated as Hs1 to 8 in this study) are boxed, and arrows indicate the direction of the half-site. The C-to-T substitution at −7833 is located within Hs6. The numbers are in reference to the transcriptional start site at +1. Schematic representations of probes containing the −7833C (ER8-WT and DR4(II)-WT) or −7833T (ER8-VT and DR4(II)-VT) allele are shown. Only nucleotides that differ from the wild-type are shown as letters; asterisks represent unchanged nucleotides. (B) EMSA was performed using *in vitro* translated VDR and RXRα. The FITC-labeled probe was incubated with VDR and RXRα as described in the Materials and methods. The complexes were resolved by electrophoresis on a 6% Long Ranger gel. This protocol was also used for the EMSAs shown in C–G. (C) EMSA was performed using *in vitro* translated TRβ and RXRα. (D) EMSA was performed using *in vitro* translated CAR. (E) EMSA was performed using *in vitro* translated CAR and RXRα. (F) EMSA was performed using *in vitro* translated PXR and RXRα. (G) We carried out the translation reaction using the empty vector, and performed EMSA using the reaction product instead of *in vitro* translated nuclear receptors, as the negative control.

Fig. 1A) [9,36]. Although the frequency of this substitution is very low (0.002), there is the possibility the −7833C>T variant may influence the transcription of the *MDR1* gene.

MDR1 mRNA expression was also induced by 2,3,7,8-tetrachlorodibenzo-p-dioxin (aryl hydrocarbon receptor (AhR) ligand) in three of seven primary human hepatocytes [37], an indication of the interindividual variation in AhR-induced expression, although the AhR responsive element (xenobiotics responsive element; XRE) in *MDR1* has not been identified. The −1211T>C (rs28746504, −1910 in Taniguchi et al., [17] and −1017 in Takane et al. [29]) SNP has been found in Japanese and Caucasian populations at allelic frequencies of 0.08–0.1 (Japanese) and 0.016 (Caucasian). The T-to-C substitution at nucleotide −1211 results in an XRE-like sequence (possible XRE, TGGTGTG>TGGCGTG, Fig. 3A) that we hypothesize may cause the interindividual variability in the response to TCDD. In addition to AhR-induced MDR1 mRNA expression, hypoxia-inducible factor-1 (HIF-1) regulates *MDR1* gene transcription [38]. The −1211T>C substitution also results in an HIF-1-responsive element (hypoxia responsive elements; HRE)-like sequence (possible HRE, GTGTG>GCGTG, Fig. 3A). However, it was unknown if HIF-1 could bind the candidate HRE in addition to the known HRE located between −49 and −45 (−53 and −49 in this study) in the promoter region of *MDR1*.

In order to clarify the functional significance of variants in the transcriptional regulatory region of *MDR1* gene, the effect of two SNPs (−7833C>T and −1211T>C) on the binding properties of nuclear receptors and on the transcriptional activity of *MDR1* was evaluated using electrophoretic mobility shift assay (EMSA) and a luciferase-reporter gene assay, respectively. The −7833C>T substitution resulted in a decrease in nuclear receptor binding and transcriptional activation *in vitro*, while the −1211T>C substitution did not produce an effect. These results suggest that the −7833C>T substitution influences the regulation of MDR1 mRNA levels through PXR, CAR, TRβ, and VDR.

2. Materials and methods

2.1. Chemicals

Rifampicin and 3-methylcholanthrene (3MC) were purchased from Wako Pure Chemicals (Osaka, Japan). $CoCl_2$, 3,3′,5-triiodo-L-thyronine (T3), and 1α,25-dihydroxyvitamin D_3 ($1,25\text{-}(OH)_2D_3$) were purchased from Sigma-Aldrich (St. Louis, MO, USA). All chemicals, except T3 and $CoCl_2$, were dissolved in dimethyl sulfoxide (DMSO). T3 and $CoCl_2$ were dissolved in 0.2 M NaOH and water, respectively.

2.2. Plasmid constructs

The expression plasmids, pDEST12.2-hPXR, pEF6/V5-hVDR, pCMVTNT-hVDR, and pcDNA3.1-TRβ, were previously constructed in our laboratory [34,35,39]. The expression plasmid encoding human RXRα cDNA (pcDNA3.1-hRXRα) was a generous gift from Dr. Shuichi Koizumi (Yamanashi University, Japan). pCMVTNT-hTRβ was constructed by ligating the *Eco*RI/*Not*I fragment from pcDNA3.1-TRβ into the pCMVTNT expression plasmid (Promega, Madison, WI, USA), which was digested with *Eco*RI and *Not*I. The pEGFP-hCAR was a generous gift from Dr. Hideto Jinno (National Institute of Health Sciences, Japan) [40]. The nucleotide at the position 540 of pEGFP-hCAR differed from the reference sequence (NM_005122) (540C>T, synonymous substitution) [40]. Thus, wild-type sequence was introduced into the pEGFP-hCAR using a QuikChange Site-Directed Mutagenesis Kit (Stratagene, La Jolla, CA, USA). pEGFP-hCAR was then digested with *Xho*I and *Eco*RI, and the resulting fragment was ligated into the pcDNA3.1/Zeo expression plasmid (Invitrogen, Carlsbad, CA, USA), which was digested with *Xho*I and *Eco*RI. This expression plasmid (pcDNA3.1-hCAR) was digested with *Xho*I and *Pme*I, and the resulting fragment was ligated into the pCMVTNT expression plasmid, which was digested with *Xho*I and *Sma*I (pCMVTNT-hCAR). The pDEST12.2-hPXR, pEF6/V5-hVDR, pcDNA3.1-TRβ, and pcDNA3.1-hCAR plasmids were used for transfections. The pDEST12.2-hPXR, pCMVTNT-hVDR, pCMVTNT-hTRβ, pCMVTNT-hCAR, and pcDNA3.1-hRXRα plasmids were used for *in vitro* synthesis.

The luciferase reporter gene plasmids, pMD10082L, pMD*824Δ90L, and pMD457L were previously constructed in our laboratory [34]. The pMD2912L plasmid was constructed by deleting the *Nsi*I fragment from pMD10082L. Mutations were introduced at positions −7833 and −1211 of pMD*824Δ90L-WT and pMD2912L-WT to create pMD*824Δ90L-VT and pMD2912L-VT, respectively, using a QuikChange Multi Site-Directed Mutagenesis Kit (Stratagene), according to the manufacturer's instructions, with the following oligonucleotides:

−7833C>T_SNP: 5′-GCTCCTGGGAGAGAGTTTATTTGAGATTAAACAAG-3′

−1211T>C_SNP: 5′-CAGGAGAATGGCGTGAACCCGGGAG-3′.

The pGL2A8-2504 [41] plasmid, which contains the XRE of the Syrian hamster CYP2A8, was digested with *Kpn*I and *Hind*III. The resulting fragment was ligated to the *Kpn*I/*Hind*III site of the firefly luciferase rapid response reporter vector pGL4.12 (Promega). This plasmid (pGL4.12-2A8) was used as a positive control.

2.3. Electrophoretic mobility shift assay (EMSA)

TNT T7 Quick Coupled Transcription/Translation Systems (Promega) were used for *in vitro* synthesis of human RXRα protein from pcDNA3.1-hRXRα, according to the manufacturer's instructions. TNT SP6 Quick Coupled Transcription/Translation Systems (Promega) were used for *in vitro* synthesis of human VDR, TRβ, CAR, and PXR proteins from pCMVTNT-hVDR, pCMVTNT-hTRβ, pCMVTNT-hCAR, and pDEST12.2-hPXR, respectively, according to the manufacturer's instructions. The plus strand sequences of probes used in the EMSAs are shown in Fig. 1A. The oligonucleotides were purchased from Sigma Genosys (Hokkaido, Japan) and equal amounts of complimentary strands were annealed. The reaction mixture was prepared as follows: a 2.5 μL aliquot of the *in vitro* translated proteins (nuclear receptor alone, or mixed at a ratio of 1:1) or unprogrammed reticulocyte lysate was incubated for 20 min at room temperature with 1 μL of 5× binding buffer (15 mM $MgCl_2$, 0.5 mM EDTA, 2.5 mM dithiothreitol (DTT), 50% glycerol and 100 mM HEPES, pH 7.75), 0.5 μL of 1 mg/mL poly(dI–dC) (GE Healthcare, Little Chalfont, UK), and 0.5 μL of 0.33 μM 5′-fluorescein isothiocyanate (FITC)-labeled double stranded oligonucleotide probe. The protein–DNA complexes were resolved by electrophoresis on 6% non-denaturing Long Ranger gels (Lonza, Rockland, ME) run in 0.5×TBE (44.5 mM Tris, 44.5 mM boric acid, and 1.25 mM EDTA) at 500 V constant voltage, and visualized and quantified on a slab gel DNA sequencer (DSQ-2000L; Shimadzu Co., Kyoto, Japan).

2.4. Cell culture

Caco-2 cells, a human colon adenocarcinoma cell line, were obtained from the American Type Culture Collection (Manassas, VA, USA). Caco-2 cells were cultured in low glucose Dulbecco's modified Eagle's medium (DMEM, Sigma-Aldrich) supplemented with 10% heat-inactivated fetal bovine serum (FBS), 100 U/mL penicillin G/100 μg/mL streptomycin (Gibco-Invitrogen, Carlsbad, CA, USA), and 1× MEM non-essential amino acids solution (Gibco-Invitrogen) at 37 °C under 5% CO_2–95% air.

2.5. Transfection and luciferase reporter gene assays

Caco-2 cells were seeded into 96-well plates (1.7×10^4 cells/well), grown overnight, and transiently transfected using HilyMax (at a ratio of DNA to HilyMax of 1:5; Dojindo Laboratories, Kumamoto, Japan)

according to the manufacturer's instructions with 10 ng/well of the indicated expression plasmid, 100 ng/well of the indicated luciferase reporter plasmid, and 10 ng/well of the *Renilla* luciferase reporter plasmid, pGL4.74 [hRluc/TK] (Promega) to normalize the transfection efficiency. After 24 h, the medium was replaced by phenol red-free DMEM (Gibco-Invitrogen) supplemented with 10% dextran-coated charcoal-stripped FBS (Hyclone Laboratories, Logan, UT, USA) containing 1 μM 3MC, 150 μM $CoCl_2$, 25 nM 1,25-$(OH)_2D_3$, 50 nM T3, 10 μM rifampicin, or vehicle (DMSO, water, or 0.2 mM NaOH) for 3.5 h except for $CoCl_2$. $CoCl_2$ treatment was performed for 6 h. Firefly and *Renilla* luciferase activities were measured using the Dual-Glo Luciferase Assay System (Promega) according to the manufacturer's instructions and a luminometer (Wallac 1420 ARVO sx Multilabel Counter, Perkin-Elmer Life Sciences, Boston, MA, USA). Firefly luciferase activity was normalized to *Renilla* luciferase activity (Luc activity). The inducibility (fold induction) was calculated as the ratio of luciferase activity of ligand-treated cells to that of control cells. As for CAR, fold transactivation was calculated as the ratio of luciferase activity of CAR-transfected cells to that of pcDNA3.1 transfected cells. The results were presented as the mean ± standard deviation (S.D.) of at least four independent experiments. The statistical analysis was performed using two-tailed, unpaired t-tests with a significance level of $P<0.05$.

3. Results

3.1. C-to-T substitution at −7833 of MDR1 decreases binding affinity of nuclear receptors to ER8 and/or DR4(II)

Nuclear receptors, such as VDR, TRβ, CAR, and PXR reportedly upregulate *MDR1* expression through the response region located 7880 to 7810 bp upstream of the *MDR1* gene. This region contains several half-sites, a pair of which composes a DR or ER (Hs1–8 in Fig. 1A). The previously reported variation −7833C>T is located within the Hs6 half-site (Fig. 1A). The effect of the C-to-T substitution at −7833 on the binding affinity of nuclear receptors to the response region was examined with EMSA using *in vitro* translated VDR, TRβ, PXR, CAR and RXRα. ER8 and DR4(II) oligonucleotide probes containing either −7833C (WT) or −7833T (VT) were used because Hs6 is involved in both ER8 and DR4(II) (Fig. 1A). The probes used for the EMSA are summarized in Fig. 1A. As described in previous reports, VDR/RXRα forms DNA–protein complexes with ER8-WT and DR4(II)-WT, with a weaker binding affinity for DR4(II) than for ER8. Introduction of the variant into the probes (DR4(II)-VT and ER8-VT) decreased the formation of VDR/RXRα and probe complexes (Fig. 1B). As described previously, the DNA-TRβ/RXRα complex was formed using DR4(II)-WT, but not with ER8-WT (Fig. 1C). The DR4(II)-TRβ/RXRα complex significantly decreased when the variant type probe (DR4(II)-VT) was used. It has been reported that CAR binds to Hs6 as a monomer [33]. Consistent with this report, the DNA–CAR monomer complex was formed with either ER8-WT or DR4(II)-WT, and the C-to-T substitution at −7833 (ER8-VT and DR4(II)-VT) caused a decrease in band formation (Fig. 1D). The CAR/RXRα DNA–protein complex was also formed when either ER8-WT or DR4(II)-WT was used as a probe, although the binding affinity of ER8-CAR/RXRα was weak (Fig. 1E). Complex formation between CAR/RXRα and the probes decreased when the WT probes were replaced with ER8-VT and DR4(II)-VT (Fig. 1E). PXR/RXRα DNA–protein complexes formed using both ER8-WT and DR4(II)-WT produced weak bands, which disappeared when ER8-VT and DR4(II)-VT were used as probes (Fig. 1F). These results indicate that the C-to-T substitution at −7833 leads to decreased binding affinity of ER8 and/or DR4(II) for VDR/RXRα, TRβ/RXRα, CAR, CAR/RXRα, and PXR/RXRα.

3.2. C-to-T substitution at −7833 of MDR1 affects the inducibility by 1,25-$(OH)_2D_3$, T3, CAR, and PXR, but does not affect the inducibility by rifampicin

The EMSA experiments revealed that the C-to-T substitution at −7833 results in decreased binding affinity of VDR/RXRα, TRβ/RXRα, CAR, CAR/RXRα, and PXR/RXRα for ER8 and/or DR4(II). To investigate the effect of the substitution on VDR-, TRβ-, CAR-, and PXR-induced *MDR1* transcription, −7833C>T was introduced into pMD*824Δ90L reporter plasmid, which contains the nuclear receptor-response region (Fig. 2A), and a luciferase reporter assay was performed using the Caco-2 intestinal epithelial cell line. In order to exclude the interaction of other nuclear receptors, we used the Caco-2 because Caco-2 cells express the nuclear receptors at relatively lower levels. As described in previous reports [34,35], 1,25-$(OH)_2D_3$ (VDR ligand) or triiodothyronine (T3, TRβ ligand) increased the luciferase activity in Caco-2 cells that were co-transfected with VDR or TRβ expression plasmid (Figs. 2B and C) although VDR or TRβ alone could not activate the transcriptional activity without the ligand (data not shown). The C-to-T substitution resulted in significantly reduced transcriptional activation by 1,25-$(OH)_2D_3$ (Fig. 2B, $P=0.0015$, unpaired t-test, two-tailed). The substitution also led to a slight decrease in T3-induced transcriptional activation, but this decrease was not significant (Fig. 2C, $P=0.0688$, unpaired t-test, two-tailed). Co-transfection of a CAR expression plasmid led to increased transcriptional activity of the reporter gene compared with the mock transfection control group (fold transactivation in Fig. 2D) due to the constitutive activity of CAR. The C-to-T substitution also partially reduced constitutive CAR transactivity (Fig. 2D, $P=0.0326$, unpaired t-test, two-tailed). Rifampicin increased transactivation of the reporter gene following transfection with the PXR expression plasmid. The −7833C>T substitution did not affect the fold induction produced by rifampicin (Fig. 2E). However, the substitution reduced both the rifampicin-dependent and -independent transcriptional activation by PXR (Fig. 2F). These results indicated that −7833C>T in the *MDR1* gene reduced the transcriptional activation which is induced by 1,25-$(OH)_2D_3$

Fig. 2. Effect of −7833C>T on the transactivation of *MDR1* by VDR, TRβ, CAR, and PXR. (A) The C-to-T mutation at −7833 was introduced into a reporter gene plasmid containing the 5′ upstream region from −7880 to −7810 bp of *MDR1* (pMD*824Δ90L). Several half-sites (designated as Hs1 to Hs8) are boxed and arrows indicate the direction of the half-site. The C-to-T substitution at −7833 is located within Hs6. The numbers are in reference to the transcriptional start site at +1. In the variant construct (pMD*824Δ90L-VT), only the nucleotide that differs from the wild-type (pMD*824Δ90L-WT) is shown as a letter; asterisks represent unchanged nucleotides. (B) Caco-2 cells were co-transfected with the indicated luciferase reporter plasmid, VDR expression plasmid, and the *Renilla* luciferase reporter plasmid, and were subsequently treated with DMSO or 1,25-$(OH)_2D_3$. Firefly luciferase activity was normalized to *Renilla* luciferase activity, and the fold induction was calculated as the ratio of luciferase activity in 1,25-$(OH)_2D_3$-treated cells to that of DMSO-treated cells. Each value represents the mean ± S.D. of independent seven experiments. Statistical analysis was performed using a two-tailed, unpaired t-test, and a statistically significant difference, as compared with the wild-type, is indicated by an asterisk (**$P<0.005$). (C) The luciferase assay was performed as described in (B) except that the TRβ expression plasmid, T3, and 0.2 mM NaOH were used instead of the VDR expression plasmid, 1,25-$(OH)_2D_3$, and DMSO, respectively. The fold induction was calculated as the ratio of luciferase activity in T3-treated cells to that in 0.2 mM NaOH-treated cells. Each value represents the mean ± S.D. of independent six experiments. Statistical analysis was performed using the two-tailed, unpaired t-test, ($P=0.069$). (D) Luciferase activity was analyzed as described in the Materials and methods. Firefly luciferase activity was normalized to *Renilla* luciferase activity, and the fold transactivation was calculated as the ratio of luciferase activity of CAR-transfected cells to that of control plasmid-transfected cells. Each value represents the mean ± S.D. of independent four experiments. Statistical analysis was performed using the two-tailed, unpaired t-test, and a statistically significant difference, as compared with the wild-type, is indicated by asterisk (*$P<0.05$). (E) The luciferase assay was performed as described in (B) except that PXR expression plasmid and rifampicin were used instead of VDR expression plasmid and 1,25-$(OH)_2D_3$, respectively. The fold induction was calculated as the ratio of luciferase activity in rifampicin-treated cells to that in DMSO-treated cells. Each value represents the mean ± S.D. of independent five experiments. (F) These data are from the experiments described in (E), but are expressed in each treatment group. The firefly luciferase activity was normalized for transfection efficiency, using the activity of co-transfected *Renilla* luciferase, and represented as Luc activity.

and T3. The −7833C>T also reduced CAR and PXR-dependent transcriptional activities.

3.3. XRE- and HRE-like sequences, resulting from a −1211T>C substitution in MDR1, are not functional

The T-to-C substitution at −1211 from the transcriptional start site of the human *MDR1* gene (−1211T>C, rs28746504) results in the formation of a XRE-like sequence (TGGTGTG>TGGCGTG, Fig. 3A). To examine the functionality of the XRE-like sequence, −1211T>C was introduced into a reporter plasmid containing the 5′ upstream region from −2912 to +117 bp of the *MDR1* gene and transfected into Caco-2 cells. The pGL4.12-2A8 construct (2A8), which contains the functional XRE, was used as the positive control [41]. As shown in Fig. 3B, 3MC (AhR ligand) did not affect transcriptional activity of Caco-2 cells transfected with either the wild-type (pMD2912L-WT) or mutated (pMD2912L-VT) construct, although the luciferase activity of the positive control reporter construct (2A8) was increased approximately 5-fold by 3MC, indicating that the XRE-like sequence containing −1211T>C is not functional.

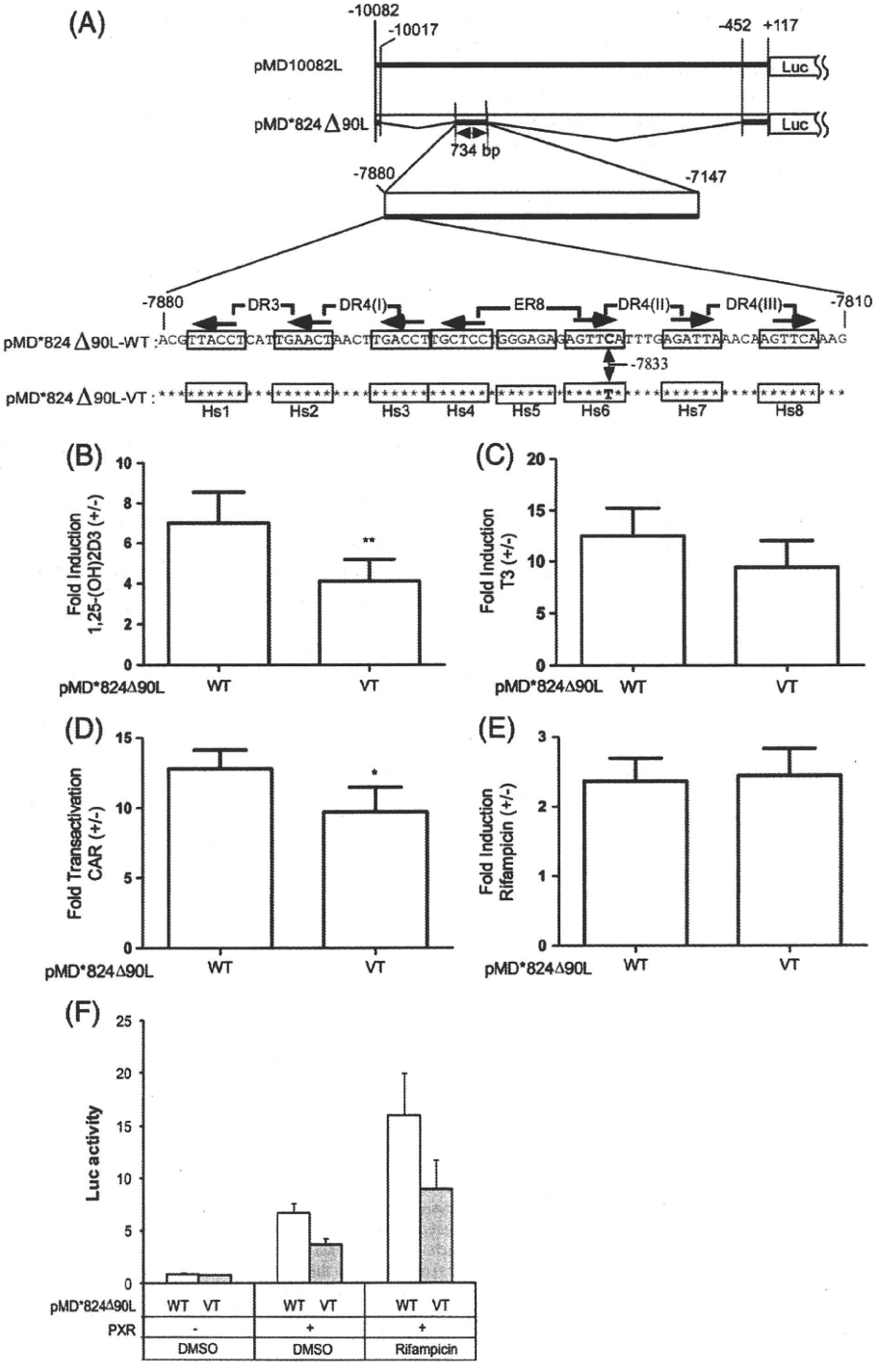

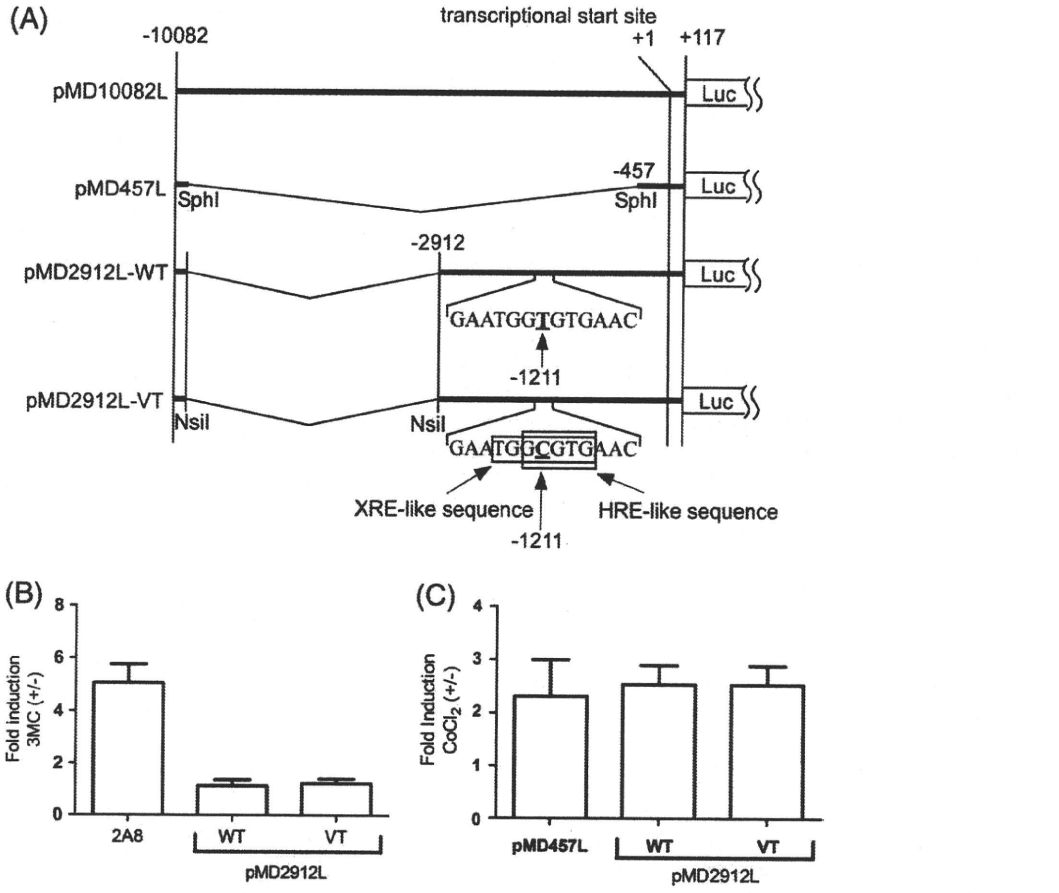

Fig. 3. Effect of −1211T>C on the transactivation of the *MDR1* gene by AhR and HIF. (A) Schematic representation of reporter plasmids containing the −1211T (pMD2912L-WT) or −1211C (pMD2912L-VT) allele. The pMD2912L plasmid was constructed by deleting the *NsiI* fragment in pMD10082L. The numbers are in reference to the transcriptional start site at +1. Xenobiotic response element (XRE)-like and hypoxia response element (HRE)-like sequences (TGGCGTG and GCGTG, respectively) resulting from the T-to-C substitution at −1211 are boxed. pMD457L was constructed by deleting the *SphI* fragment from pMD10082L. (B) Caco-2 cells were co-transfected with the indicated luciferase reporter plasmid and the *Renilla* luciferase reporter plasmid, and were subsequently treated with DMSO or 3MC as described in Materials and methods. Firefly luciferase activity was normalized to *Renilla* luciferase activity, and the fold induction was calculated as the ratio of luciferase activity in 3MC-treated cells to that in DMSO-treated cells. As a positive control, pGL4.12-2A8 (2A8), which contains the functional XRE of Syrian hamster CYP2A8, was used. Each value represents the mean ± S.D. of four independent experiments. (C) Caco-2 cells were co-transfected with the indicated luciferase reporter plasmid and the *Renilla* luciferase reporter plasmid, and then replaced by media with or without $CoCl_2$ as described in Materials and methods. Firefly luciferase activity was normalized to *Renilla* luciferase activity, and the fold induction was calculated as the ratio of luciferase activity in $CoCl_2$-treated cells to that of untreated cells. The pMD457L, which contains the functional HRE but does not contain the HRE-like sequence, was used as a control. Each value represents the mean ± S.D. of four independent experiments.

The T-to-C substitution at −1211 also results in the formation of an HRE-like sequence (GTGTG>GCGTG, Fig. 3A). The effect of the −1211T>C mutation on hypoxia responsiveness was measured by transfecting Caco-2 cells with the pMD2912L-WT or pMD2912L-VT. The cells were cultured with or without $CoCl_2$, a hypoxia-mimetic agent [38]. As shown in Fig. 3C, $CoCl_2$-dependent inducibility of the wild-type construct (pMD2912L-WT) was similar to that of the variant construct (pMD2912L-VT). Moreover, the inducibility of the wild-type construct, which includes the HRE-like sequence and the known HRE between −53 and −49, was also similar to that of pMD457L, which contains the reported functional HRE alone [38]. Therefore, the −1211T>C substitution did not affect the hypoxic response, and the HRE-like sequence is also non-functional.

4. Discussion

Many studies have tried to clarify the relationship between P-gp expression levels and SNPs located in the coding and transcriptional regulatory regions of *MDR1* [2,19,21–23,28,42]. However, most of these studies have not explored the functionality of these SNPs based on the nuclear receptor-responsive elements that play important roles in the expression of MDR1 mRNA. Therefore, the proposed functions of SNPs in the 5′-flanking region, such as −129T>C, remain controversial [27,30,31]. In this study, we analyzed the SNP located in the nuclear receptor-responsive region of *MDR1* and the SNP that results in conversion to a potential nuclear receptor-responsive element. The −7833C>T substitution, located in the nuclear receptor-responsive region, was found to significantly decrease the binding affinity of VDR/RXRα, TRβ/RXRα, CAR, CAR/RXRα, and PXR/RXRα (Fig. 1). In addition, the −7833C>T substitution reduced the transcriptional activation induced by $1,25\text{-}(OH)_2D_3$ and T3, and suppressed CAR and PXR-dependent transcriptional activities *in vitro* (Fig. 2).

Recently, we reported that the relative binding ability of VDR/RXRα to the elements located in this region is: DR4(I)>DR3>ER8(MdC3)>DR4(III)>DR4(II), and DR4(I), with ER8(MdC3), and DR4(III) the main players in VDR-mediated MDR1 induction [35]. Since −7833C>T is involved in ER8(MdC3) (Fig. 1A), and ER8(MdC3) contributes to VDR-mediated MDR1 induction [35], it is possible that the −7833C>T substitution decreases VDR-mediated MDR1 mRNA induction through ER8(MdC3). We also previously indicated that TRβ/RXRα bound to several DRs in the order: DR4(I)>DR4(II)>DR3≈DR4(III), and that every direct repeat contributes to TRβ-

mediated MDR1 induction [34]. Since −7833C>T is located in DR4(II) (Fig. 1A), and TRβ/RXRα can bind to DR4(II) at a relative high affinity [34], it is reasonable that the −7833C>T substitution could affect TRβ-mediated MDR1 mRNA induction though DR4(II). Burk et al. reported that CAR binds DR4(I) and DR4(III) as a heterodimer with RXRα, and to the 5′ half-site of DR4(II) (designated as Hs6 in Fig. 1A) as a CAR monomer, and suggested that DR4(I) and the 5′ half-site of DR4(II) (Hs6) were important elements for the CAR-mediated MDR1 induction [33]. In this study, the CAR monomer formed a complex with Hs6 both in ER8(MdC3) and DR4(II), and CAR/RXRα formed a complex with DR4(II) (Figs. 1D and E). These results and those of Burk indicate that Hs6 contributes to the CAR-mediated MDR1 mRNA induction. Since −7833C>T is found in Hs6 and DR4(II) (Fig. 1A), the −7833C>T substitution could decrease CAR-mediated MDR1 mRNA induction (Fig. 2D) even if the CAR monomer or CAR/RXRα contributes to MDR1 mRNA induction. Geick et al. reported that PXR/RXRα bind to DR4(I), DR4(II), and DR4(III) in the nuclear receptor-responsive elements of *MDR1*, with the highest affinity for DR4(III). DR4(I) is involved in rifampicin-mediated induction by PXR [32]. They suggest that DR4(II) does not contribute to the rifampicin-mediated induction by PXR even if the PXR/RXRα can bind DR4(II). In our study, PXR/RXRα formed a weak complex with DR4(II), and the −7833C>T substitution decreased the binding affinity of PXR/RXRα to DR4(II) (Fig. 1F). The −7833C>T substitution also decreased the transcriptional activation by PXR both in the presence and absence of rifampicin (Fig. 2F), but fold induction of MDR1 mRNA by rifampicin was not affected (Fig. 2E). These results suggest that DR4(II) does not contribute to rifampicin-activated MDR1 mRNA induction by PXR, which was consistent with previous observations [32]. PXR-dependent *MDR1* gene transcription without rifampicin was observed not only in this study, but also in other reports [32,43,44], and PXR-dependent CYP3A4 gene transcription without rifampicin also has been reported [32,43,44]. Since the −7833C>T substitution decreased PXR-dependent basal activation without rifampicin (Fig. 2F), DR4(II), which contains −7833C>T, may be involved in PXR-dependent basal MDR1 expression, not ligand-dependent expression. Although −7833C>T affected nuclear receptor (VDR, TRβ, CAR, and PXR)-mediated *MDR1* gene transactivation, it suppressed only about one third of total transactivity in each nuclear receptor (Fig. 2). We propose that this partial inhibition may be due to the multiple responsive elements that mediate MDR1 mRNA induction. Since xenobiotics and endogenous substrates-activated P-gp inductions play key roles in physiological functions [1,4,11,45], nuclear receptors might stimulate *MDR1* transcription through the multiple responsive elements.

Since the T-to-C substitution at nucleotide −1211 forms an XRE-like sequence (Fig. 3A) and AhR-induced MDR1 expression shows interindividual variation in human hepatocytes [37,46], we hypothesized that the −1211T>C substitution could affect the interindividual variation in MDR1 mRNA expression. However, AhR-dependent *MDR1* activation was not observed with either −1211T or −1211C (Fig. 3B), indicating that the −1211T>C substitution does not form a functional XRE. The −1211T>C substitution also forms an HRE-like sequence (Fig. 3A), and the −129T>C substitution, which is completely linkage disequilibrated with −1211T>C in Japanese [27,31], reportedly affects the expression level of MDR1 mRNA in intestine and colon cancer cells. Since the concentrations of oxygen in the intestine and cancer cells are relatively low compared to other tissues [30], it is possible that the −1211T>C substitution affects the HIF-induced MDR1 expression in a synergistic or inhibitory manner. However, the −1211T>C substitution could not affect the MDR1 expression, which was induced by a chemically-induced hypoxic condition, indicating that the −1211T>C substitution could not form the functional HRE (Fig. 3C).

In summary, we have demonstrated that the −7833C>T substitution in the *MDR1* gene decreases the binding affinities of nuclear receptors, VDR/RXRα, TRβ/RXRα, CAR, CAR/RXRα, and PXR/RXRα, to their responsive elements located around −7833. We also showed that the C-to-T substitution at −7833 reduces transcriptional activation of *MDR1* by VDR, TRβ, CAR, and PXR. However, another SNP at −1211 (T>C), which forms XRE-like and HRE-like sequences, failed to affect the AhR-dependent and hypoxia-induced *MDR1* transcriptional activation. Although the frequency of −7833C>T substitution in the *MDR1* gene is relatively low, knowledge of the −7833C>T substitution in *MDR1* is crucial for subjects who hold the −7833T allele because the pharmacokinetics of P-gp substrates may differ from wild-type profile. Further study, especially clinical studies, is necessary to confirm the functional significance of the −7833C>T substitution in the interindividual differences in P-gp expression level.

Acknowledgments

We thank Prof. Shuichi Koizumi (Yamanashi University, Japan) and Dr. Hideo Jinno (National Institute of Health Sciences, Japan) for providing the human RXRα cDNA and human CAR cDNA, respectively. This work was supported in part by grants from the Ministry of Health, Labor and Welfare of Japan (to M.T.) and the Japan Health Sciences Foundation (Research on Publicly Essential Drugs and Medical Devices) (to K.K.).

References

[1] V.J. Wacher, J.A. Silverman, Y. Zhang, L.Z. Benet, Role of P-glycoprotein and cytochrome P450 3A in limiting oral absorption of peptides and peptidomimetics, J. Pharm. Sci. 87 (1998) 1322–1330.
[2] T. Sakaeda, T. Nakamura, K. Okumura, MDR1 genotype-related pharmacokinetics and pharmacodynamics, Biol. Pharm. Bull. 25 (2002) 1391–1400.
[3] F. Thiebaut, T. Tsuruo, H. Hamada, M.M. Gottesman, I. Pastan, M.C. Willingham, Cellular localization of the multidrug-resistance gene product P-glycoprotein in normal human tissues, Proc. Natl Acad. Sci. USA 84 (1987) 7735–7738.
[4] M. Thorn, N. Finnstrom, S. Lundgren, A. Rane, L. Loof, Cytochromes P450 and MDR1 mRNA expression along the human gastrointestinal tract, Br. J. Clin. Pharmacol. 60 (2005) 54–60.
[5] C. Cordon-Cardo, J.P. O'Brien, D. Casals, L. Rittman-Grauer, J.L. Biedler, M.R. Melamed, J.R. Bertino, Multidrug-resistance gene (P-glycoprotein) is expressed by endothelial cells at blood–brain barrier sites, Proc. Natl Acad. Sci. USA 86 (1989) 695–698.
[6] P.B. Watkins, The barrier function of CYP3A4 and P-glycoprotein in the small bowel, Adv. Drug Deliv. Rev. 27 (1997) 161–170.
[7] J. Taipalensuu, H. Tornblom, G. Lindberg, C. Einarsson, F. Sjoqvist, H. Melhus, P. Garberg, B. Sjostrom, B. Lundgren, P. Artursson, Correlation of gene expression of ten drug efflux proteins of the ATP-binding cassette transporter family in normal human jejunum and in human intestinal epithelial Caco-2 cell monolayers, J. Pharmacol. Exp. Ther. 299 (2001) 164–170.
[8] C. Zimmermann, H. Gutmann, P. Hruz, J.P. Gutzwiller, C. Beglinger, J. Drewe, Mapping of multidrug resistance gene 1 and multidrug resistance-associated protein isoform 1 to 5 mRNA expression along the human intestinal tract, Drug Metab. Dispos. 33 (2005) 219–224.
[9] K. Sai, N. Kaniwa, M. Itoda, Y. Saito, R. Hasegawa, K. Komamura, K. Ueno, S. Kamakura, M. Kitakaze, K. Shirao, H. Minami, A. Ohtsu, T. Yoshida, N. Saijo, Y. Kitamura, N. Kamatani, S. Ozawa, J. Sawada, Haplotype analysis of ABCB1/MDR1 blocks in a Japanese population reveals genotype-dependent renal clearance of irinotecan, Pharmacogenetics 13 (2003) 741–757.
[10] K.N. Faber, M. Muller, P.L. Jansen, Drug transport proteins in the liver, Adv. Drug Deliv. Rev. 55 (2003) 107–124.
[11] A. Doran, R.S. Obach, B.J. Smith, N.A. Hosea, S. Becker, E. Callegari, C. Chen, X. Chen, E. Choo, J. Cianfrogna, L.M. Cox, J.P. Gibbs, M.A. Gibbs, H. Hatch, C.E. Hop, I.N. Kasman, J. Laperle, J. Liu, X. Liu, M. Logman, D. Maclin, F.M. Nedza, F. Nelson, E. Olson, S. Rahematpura, D. Raunig, S. Rogers, K. Schmidt, D.K. Spracklin, M. Szewc, M. Troutman, E. Tseng, M. Tu, J.W. Van Deusen, K. Venkatakrishnan, G. Walens, E.Q. Wang, D. Wong, A.S. Yasgar, C. Zhang, The impact of P-glycoprotein on the disposition of drugs targeted for indications of the central nervous system: evaluation using the MDR1A/1B knockout mouse model, Drug Metab. Dispos. 33 (2005) 165–174.
[12] N.H. Hendrikse, A.H. Schinkel, E.G. de Vries, E. Fluks, W.T. Van der Graaf, A.T. Willemsen, W. Vaalburg, E.J. Franssen, Complete in vivo reversal of P-glycoprotein pump function in the blood–brain barrier visualized with positron emission tomography, Br. J. Pharmacol. 124 (1998) 1413–1418.
[13] M.B. Muller, M.E. Keck, E.B. Binder, A.E. Kresse, T.P. Hagemeyer, R. Landgraf, F. Holsboer, M. Uhr, ABCB1 (MDR1)-type P-glycoproteins at the blood–brain barrier modulate the activity of the hypothalamic-pituitary-adrenocortical system: implications for affective disorder, Neuropsychopharmacology 28 (2003) 1991–1999.

[14] E.G. Schuetz, K.N. Furuya, J.D. Schuetz, Interindividual variation in expression of P-glycoprotein in normal human liver and secondary hepatic neoplasms, J. Pharmacol. Exp. Ther. 275 (1995) 1011–1018.
[15] K.S. Lown, R.R. Mayo, A.B. Leichtman, H.L. Hsiao, D.K. Turgeon, P. Schmiedlin-Ren, M.B. Brown, W. Guo, S.J. Rossi, L.Z. Benet, P.B. Watkins, Role of intestinal P-glycoprotein (mdr1) in interpatient variation in the oral bioavailability of cyclosporine, Clin. Pharmacol. Ther. 62 (1997) 248–260.
[16] A. Asghar, J.C. Gorski, B. Haehner-Daniels, S.D. Hall, Induction of multidrug resistance-1 and cytochrome P450 mRNAs in human mononuclear cells by rifampin, Drug Metab. Dispos. 30 (2002) 20–26.
[17] S. Taniguchi, Y. Mochida, T. Uchiumi, T. Tahira, K. Hayashi, K. Takagi, M. Shimada, Y. Maehara, H. Kuwano, S. Kono, H. Nakano, M. Kuwano, M. Wada, Genetic polymorphism at the 5′ regulatory region of multidrug resistance 1 (MDR1) and its association with interindividual variation of expression level in the colon, Mol. Cancer Ther. 2 (2003) 1351–1359.
[18] R. Kerb, A.S. Aynacioglu, J. Brockmoller, R. Schlagenhaufer, S. Bauer, T. Szekeres, A. Hamwi, M. Fritzer-Szekeres, C. Baumgartner, H.Z. Ongen, P. Guzelbey, I. Roots, U. Brinkmann, The predictive value of MDR1, CYP2C9, and CYP2C19 polymorphisms for phenytoin plasma levels, Pharmacogenomics J. 1 (2001) 204–210.
[19] U. Brinkmann, M. Eichelbaum, Polymorphisms in the ABC drug transporter gene MDR1, Pharmacogenomics J. 1 (2001) 59–64.
[20] S. Saito, A. Iida, A. Sekine, Y. Miura, C. Ogawa, S. Kawauchi, S. Higuchi, Y. Nakamura, Three hundred twenty-six genetic variations in genes encoding nine members of ATP-binding cassette, subfamily B (ABCB/MDR/TAP), in the Japanese population, J. Hum. Genet. 47 (2002) 38–50.
[21] R.B. Kim, B.F. Leake, E.F. Choo, G.K. Dresser, S.V. Kubba, U.I. Schwarz, A. Taylor, H.G. Xie, J. McKinsey, S. Zhou, L.B. Lan, J.D. Schuetz, E.G. Schuetz, G.R. Wilkinson, Identification of functionally variant MDR1 alleles among European Americans and African Americans, Clin. Pharmacol. Ther. 70 (2001) 189–199.
[22] C. Kimchi-Sarfaty, J.M. Oh, I.W. Kim, Z.E. Sauna, A.M. Calcagno, S.V. Ambudkar, M.M. Gottesman, A "silent" polymorphism in the MDR1 gene changes substrate specificity, Science 315 (2007) 525–528.
[23] S. Hoffmeyer, O. Burk, O. von Richter, H.P. Arnold, J. Brockmoller, A. Johne, I. Cascorbi, T. Gerloff, I. Roots, M. Eichelbaum, U. Brinkmann, Functional polymorphisms of the human multidrug-resistance gene: multiple sequence variations and correlation of one allele with P-glycoprotein expression and activity in vivo, Proc. Natl Acad. Sci. USA 97 (2000) 3473–3478.
[24] D. Wang, A.D. Johnson, A.C. Papp, D.L. Kroetz, W. Sadee, Multidrug resistance polypeptide 1 (MDR1, ABCB1) variant 3435C>T affects mRNA stability, Pharmacogenet. Genomics 15 (2005) 693–704.
[25] T. Sakaeda, T. Nakamura, M. Horinouchi, M. Kakumoto, N. Ohmoto, T. Sakai, Y. Morita, T. Tamura, N. Aoyama, M. Hirai, M. Kasuga, K. Okumura, MDR1 genotype-related pharmacokinetics of digoxin after single oral administration in healthy Japanese subjects, Pharm. Res. 18 (2001) 1400–1404.
[26] N. Morita, T. Yasumori, K. Nakayama, Human MDR1 polymorphism: G2677T/A and C3435T have no effect on MDR1 transport activities, Biochem. Pharmacol. 65 (2003) 1843–1852.
[27] Y. Moriya, T. Nakamura, M. Horinouchi, T. Sakaeda, T. Tamura, N. Aoyama, T. Shirakawa, A. Gotoh, S. Fujimoto, M. Matsuo, M. Kasuga, K. Okumura, Effects of polymorphisms of MDR1, MRP1, and MRP2 genes on their mRNA expression levels in duodenal enterocytes of healthy Japanese subjects, Biol. Pharm. Bull. 25 (2002) 1356–1359.
[28] B. Wang, S. Ngoi, J. Wang, S.S. Chong, C.G. Lee, The promoter region of the MDR1 gene is largely invariant, but different single nucleotide polymorphism haplotypes affect MDR1 promoter activity differently in different cell lines, Mol. Pharmacol. 70 (2006) 267–276.
[29] H. Takane, D. Kobayashi, T. Hirota, J. Kigawa, N. Terakawa, K. Otsubo, I. Ieiri, Haplotype-oriented genetic analysis and functional assessment of promoter variants in the MDR1 (ABCB1) gene, J. Pharmacol. Exp. Ther. 311 (2004) 1179–1187.
[30] T. Koyama, T. Nakamura, C. Komoto, T. Sakaeda, M. Taniguchi, N. Okamura, T. Tamura, N. Aoyama, T. Kamigaki, Y. Kuroda, M. Kasuga, K. Kadoyama, K. Okumura, MDR1 T-129C polymorphism can be predictive of differentiation, and thereby prognosis of colorectal adenocarcinomas in Japanese, Biol. Pharm. Bull. 29 (2006) 1449–1453.
[31] W. Qian, M. Homma, F. Itagaki, H. Tachikawa, Y. Kawanishi, K. Mizukami, T. Asada, S. Inomata, K. Honda, N. Ohkohchi, Y. Kohda, MDR1 gene polymorphism in Japanese patients with schizophrenia and mood disorders including depression, Biol. Pharm. Bull. 29 (2006) 2446–2450.
[32] A. Geick, M. Eichelbaum, O. Burk, Nuclear receptor response elements mediate induction of intestinal MDR1 by rifampin, J. Biol. Chem. 276 (2001) 14581–14587.
[33] O. Burk, K.A. Arnold, A. Geick, H. Tegude, M. Eichelbaum, A role for constitutive androstane receptor in the regulation of human intestinal MDR1 expression, Biol. Chem. 386 (2005) 503–513.
[34] K. Kurose, M. Saeki, M. Tohkin, R. Hasegawa, Thyroid hormone receptor mediates human MDR1 gene expression—identification of the response region essential for gene expression, Arch. Biochem. Biophys. 474 (2008) 82–90.
[35] M. Saeki, K. Kurose, M. Tohkin, R. Hasegawa, Identification of the functional vitamin D response elements in the human MDR1 gene, Biochem. Pharmacol. 76 (2008) 531–542.
[36] K. Sai, M. Itoda, Y. Saito, K. Kurose, N. Katori, N. Kaniwa, K. Komamura, T. Kotake, H. Morishita, H. Tomoike, S. Kamakura, M. Kitakaze, T. Tamura, N. Yamamoto, H. Kunitoh, Y. Yamada, Y. Ohe, Y. Shimada, K. Shirao, H. Minami, A. Ohtsu, T. Yoshida, N. Saijo, N. Kamatani, S. Ozawa, J. Sawada, Genetic variations and haplotype structures of the ABCB1 gene in a Japanese population: an expanded haplotype block covering the distal promoter region, and associated ethnic differences, Ann. Hum. Genet. 70 (2006) 605–622.
[37] E. Jigorel, M. Le Vee, C. Boursier-Neyret, Y. Parmentier, O. Fardel, Differential regulation of sinusoidal and canalicular hepatic drug transporter expression by xenobiotics activating drug-sensing receptors in primary human hepatocytes, Drug Metab. Dispos. 34 (2006) 1756–1763.
[38] K.M. Comerford, T.J. Wallace, J. Karhausen, N.A. Louis, M.C. Montalto, S.P. Colgan, Hypoxia-inducible factor-1-dependent regulation of the multidrug resistance (MDR1) gene, Cancer Res. 62 (2002) 3387–3394.
[39] S. Koyano, Y. Saito, H. Fukushima-Uesaka, S. Ishida, S. Ozawa, N. Kamatani, H. Minami, A. Ohtsu, T. Hamaguchi, K. Shirao, T. Yoshida, N. Saijo, H. Jinno, J. Sawada, Functional analysis of six human aryl hydrocarbon receptor variants in a Japanese population, Drug Metab. Dispos. 33 (2005) 1254–1260.
[40] H. Jinno, T. Tanaka-Kagawa, N. Hanioka, S. Ishida, M. Saeki, A. Soyama, M. Itoda, T. Nishimura, Y. Saito, S. Ozawa, M. Ando, J. Sawada, Identification of novel alternative splice variants of human constitutive androstane receptor and characterization of their expression in the liver, Mol. Pharmacol. 65 (2004) 496–502.
[41] K. Kurose, M. Tohkin, M. Fukuhara, A novel positive regulatory element that enhances hamster CYP2A8 gene expression mediated by xenobiotic responsive element, Mol. Pharmacol. 55 (1999) 279–287.
[42] J.M. Gow, L.W. Chinn, D.L. Kroetz, The effects of ABCB1 3′-untranslated region variants on mRNA stability, Drug Metab. Dispos. 36 (2008) 10–15.
[43] A. Pfrunder, H. Gutmann, C. Beglinger, J. Drewe, Gene expression of CYP3A4, ABC-transporters (MDR1 and MRP1-MRP5) and hPXR in three different human colon carcinoma cell lines, J. Pharm. Pharmacol. 55 (2003) 59–66.
[44] L. Cerveny, L. Svecova, E. Anzenbacherova, R. Vrzal, F. Staud, Z. Dvorak, J. Ulrichova, P. Anzenbacher, P. Pavek, Valproic acid induces CYP3A4 and MDR1 gene expression by activation of constitutive androstane receptor and pregnane X receptor pathways, Drug Metab. Dispos. 35 (2007) 1032–1041.
[45] S. Marchetti, R. Mazzanti, J.H. Beijnen, J.H. Schellens, Concise review: clinical relevance of drug–drug and herb–drug interactions mediated by the ABC transporter ABCB1 (MDR1, P-glycoprotein), Oncologist 12 (2007) 927–941.
[46] P. Olinga, M.G. Elferink, A.L. Draaisma, M.T. Merema, J.V. Castell, G. Perez, G.M. Groothuis, Coordinated induction of drug transporters and phase I and II metabolism in human liver slices, Eur. J. Pharm. Sci. 33 (2008) 380–389.

Drug Metab. Pharmacokinet. 25 (2): 180–189 (2010).

Regular Article

Construction of a System that Simultaneously Evaluates CYP1A1 and CYP1A2 Induction in a Stable Human-derived Cell Line using a Dual Reporter Plasmid

Wataru SATO[1], Hiroyuki SUZUKI[1], Takamitsu SASAKI[1,*], Takeshi KUMAGAI[1], Shuhei SAKAGUCHI[1], Michinao MIZUGAKI[2], Shinichi MIYAIRI[3], Yasushi YAMAZOE[4] and Kiyoshi NAGATA[1]

[1]*Department of Environmental and Health Science, Tohoku Pharmaceutical University, Sendai, Japan*
[2]*Department of Clinical Pharmaceutics, Tohoku Pharmaceutical University, Sendai, Japan*
[3]*Laboratory of Bio-organic Chemistry, College of Pharmacy, Nihon University, Chiba, Japan*
[4]*Division of Drug Metabolism and Molecular Toxicology, Graduate School of Pharmaceutical Sciences, Tohoku University, Sendai, Japan*

Full text of this paper is available at http://www.jstage.jst.go.jp/browse/dmpk

Summary: Human *CYP1A1* and *CYP1A2* genes are in a head-to-head orientation on chromosome 15 and are separated by a 23-kb intergenic space. To our knowledge, this is the first report on a stable cell line that contains the 23-kb full-length regulatory region and is able to simultaneously assess the transcriptional activation of *CYP1A1* and *CYP1A2* genes. The stable cell line that constitutively expresses the reporter activities was constructed by inserting the dual reporter plasmid containing the 23-kb region between the *CYP1A1* and *CYP1A2* genes into the chromosome. Transcriptional activation of the *CYP1A1* and *CYP1A2* genes was measured simultaneously using luciferase (Luc) and secreted alkaline phosphatase (SEAP) activities, respectively. To demonstrate the utility of the stable cell line, CYP1A1/1A2 induction by the majority of compounds previously identified as CYP1A1/1A2 inducers was measured. The results clearly show that all compounds caused induction of reporter activities. In addition to assessing transcriptional activation of the *CYP1A1* and *CYP1A2* genes by measuring reporter activities, we determined the intrinsic CYP1A1 and CYP1A2 mRNA levels by treating them with the same compounds. The results suggest that this stable cell line may be used to rapidly and accurately predict CYP1A1/1A2 induction.

Keywords: CYP1A1; CYP1A2; XRE; AhR; in vitro reporter assay; stably cell line

Introduction

In humans, the CYP1A subfamily is comprised of 2 members—*CYP1A1* and *CYP1A2*. CYP1A1 and CYP1A2 in the liver play important roles in the detoxification of therapeutic agents and environmental chemicals. These enzymes are also responsible for the metabolic activation of polycyclic aromatic hydrocarbons (PAHs) and aromatic amines that are present in combustion products such as cigarette smoke and charcoal-grilled foods.[1)] CYP1A1 and CYP1A2 are induced by exposure to various chemicals including halogenated hydrocarbons such as 2,3,7,8-tetrachlorodibenzo-*p*-dioxin (TCDD) or PAHs such as benzo[*a*]pyrene (B[*a*]P) and 3-methylcholanthrene (3-MC).[2,3)] Induction of CYP1A1 and CYP1A2 is under the regulatory control of the aryl hydrocarbon receptor (AhR). Ligand-activated AhR translocates into the nucleus and heterodimerizes with the AhR nuclear translocator (ARNT). The ligand-AhR-ARNT complex then binds to the regulatory *cis*-element xenobiotic-responsive element (XRE), which locates the upstream portion of target genes to activate their transcription.[2-5)]

The Food and Drug Administration (FDA) currently suggests that the most reliable method to study induction potency of drugs is by using a primary culture of human hepatocytes that represents the entire repertoire of hepatic drug metabolism enzymes and the genes for maintaining liver-specific functions.[6)] However, this method frequently shows large donor-to-donor variability in induction response, resulting in difficulties in data in-

Received; December 24, 2009, Accepted; January 20, 2010
**To whom correspondence should be addressed:* Takamitsu SASAKI, *Department of Environmental and Health Science, Tohoku Pharmaceutical University, 4-4-1, Komatsushima, Aoba-ku, Sendai 981-8558, Japan. Tel. +81-22-727-0134, Fax. +81-275-2013, E-mail: t-sasaki@tohoku-pharm.ac.jp*

terpretation.[7] Furthermore, the expression of many proteins has been shown to decrease rapidly during cultivation of human hepatocytes, with drug metabolism enzymes being particularly sensitive.[8] Another disadvantage of using human hepatocytes is their high cost.[9] Thus, the use of human hepatocytes is restricted, and limited access to suitable tissue samples prevents their use in high-throughput screening systems.

Recently, rapid and sensitive bioassays of CYP1A1/1A2 induction are mainly based on application of a luciferase (Luc) gene reporter plasmid that includes the transcriptional regulatory regions of *CYP1A1* and *CYP1A2* genes, respectively. These bioassays require transient transfection of the plasmid DNA construct before each experiment. Consequently, this is difficult to apply in high-throughput screening systems. Additionally, the data often varies between experiments because controlling transfection efficiency is difficult. On the other hand, several researchers have reported on cell-based high-throughput screening systems to assess the induction of CYP1A1 using stable reporter gene expression, which has improved problems associated with the transient expression of the plasmid gene.[10] These systems are constructed by inserting the reporter gene into chromosomes of liver-derived cell lines such as HepG2. The reporter cell lines are then easily maintained as HepG2, and the culture conditions are simpler than those required by hepatocytes. Thus, these stable reporter gene expression systems have the advantage of being more readily available and reproducible than the transient expression systems or hepatocytes used for assessment of CYP1A1/1A2 induction.

The sequence and genomic orientation of the *CYP1A1* and *CYP1A2* loci on chromosome 15 have been reported.[11] The *CYP1A1* and *CYP1A2* genes are located immediately adjacent to each other in a head-to-head orientation. The 2 genes are separated by more than 20-kb of intervening DNA, which possesses 13 candidates for XRE. Yueh *et al.* and Chao *et al.* have been using established stable cell lines harboring a Luc reporter gene integrated in artificial multiple XREs.[10,12] In addition, another reporter cell line has stably integrated approximately 1.6-kb of the 5′-flanking region of the *CYP1A1* gene.[13] In contrast, assessment systems of CYP1A2 induction using stable reporter gene expression remain to be established. We have reported that transcriptional activation of the *CYP1A1* and *CYP1A2* genes is regulated simultaneously through a common regulatory element existing between these 2 genes that act bidirectionally.[14] Thus, transcriptional activation of *CYP1A1* and *CYP1A2* genes is necessary to assess its intensity in a simultaneous measurement method. Furthermore, to reflect the induction *in vivo*, it is important to establish stable cell lines containing the reporter genes and the 23-kb intergenic spacer regions between *CYP1A1* and *CYP1A2* genes. However, current procedures are not assessed under such conditions.

To develop a simultaneous evaluation method for CYP1A1/1A2 induction, we established a stable reporter gene expression in HepG2 for high-throughput screening systems. Stable reporter cell lines are designed to simultaneously assess the transcriptional activation of *CYP1A1* and *CYP1A2* genes and target the full-length regulatory region existing between these 2 genes. In the present study, this system was used to determine whether known CYP1A1/1A2 inducers, such as drugs, endogenous compounds, and PAHs, mediate induction of CYP1A1/1A2.

Materials and Methods

Materials: 3-MC, benzo[*e*]pyrene (B[*e*]P), benz[*a*]anthracene (B[*a*]A), omeprazole (OME), lansoprazole (LPZ), and albendazole (ALB) were purchased from Sigma-Aldrich (St. Louis, MO, USA). α-Naphthoflavone (α-NF), β-naphthoflavone (β-NF), B[*a*]P, 9,10-dihydroanthracene (DHA), 7-methylbenz[*a*]anthracene (7-MB[*a*]A), dibenz[*de,kl*]anthracene (DB[*de,kl*]A), chrysene (Chr), dibenz[*a,h*]anthracene (DB[*a,h*]A), and dibenz[*a,c*]anthracene (DB[*a,c*]A) were obtained from Tokyo Chemical Industry (Tokyo, Japan). TCDD and dibenz[*a,j*]acrydine (DB[*a,j*]AC) was purchased from Wako Pure Chemicals (Osaka, Japan) and dimethylsulfoxide (DMSO) from Nacalai Tesque (Kyoto, Japan). Indirubin (IND) was synthesized as descrived by Hossel *et al.* (1999).[15]

Generation of stable cell lines and cell extract: The dual reporter plasmids of human *CYP1A1* and *CYP1A2* (pd-1A1/1A2) containing approximately 23-kb of DNA segments (from +1039 of the *CYP1A1* gene to +90 of the *CYP1A2* gene) were reported previously.[14] The plasmids pd-1A1/1A2 and pQBI including the neomycin resistant gene (Wako Pure Chemicals) were linearized with *Not*I (NIPPON GENE, Tokyo, Japan), and the resulting fragments were mixed at a molar ratio of 5:1 and ligated using DNA ligation Kit ver. 2.1 (TaKaRa Bio, Kyoto, Japan). The human hepatoma cell line HepG2 was obtained from the RIKEN cell bank (Tsukuba, Japan) and cultured in Dulbecco's modified Eagle's medium (DMEM, WAKO Pure Chemicals) supplemented with 10% fetal calf serum (Biowest. Miami, FL, USA) and MEM nonessential amino acids (Invitrogen, Carlsbad, CA, USA). Cells were seeded in 6-well tissue culture plates (BD Biosciences, Heidelberg, Germany) at 3×10^5 cells per well a day before transfection, and the ligation fragment was transfected using Targefect F-1 (TARGETING SYSTEM, El Cajon, CA, USA) according to the manufacturer's instructions. After 2-weeks incubation, the cells were selected with 700–900 μg/mL geneticin (G418, Invitrogen). Medium was changed 3 times for 3 weeks until small colonies were visible. Five out of 12 colonies were further subcloned into 48-well tissue culture plates (BD Biosciences) to obtain monoclonal cells.

G418-resistant clones were chosen for induction testing by treating the cells with 1 μM 3-MC and 10 μM β-NF. The induction response was measured using the Luc and secreted alkaline phosphatase (SEAP) assay method. A clone exhibiting the greatest induction response was selected for this study.

Cell culture and cell extract: A stable cell line was cultured in DMEM containing 10% fetal calf serum, MEM nonessential amino acids, and antibiotic-antimycotic (Invitrogen). The cells were seeded in 24-well tissue culture plates (BD Biosciences) at 1×10^5 cells per well in 0.5 mL of DMEM, and the media containing the various compounds dissolved in DMSO (final concentration, 0.1%) were changed at 24 h intervals. Control cells were treated with 0.1% DMSO. After 48 h exposure to various xenochemicals, portions of the media were collected and used for the SEAP assay. Subsequently, cells were washed with phosphate buffered saline (PBS) and suspended in 0.1 mL of Passive Lysis Buffer (Promega, Madison, MI, USA) in a microcentrifuge tube. The cell suspension was centrifuged at $12,000 \times g$ for 5 minutes at 4°C. The supernatant was processed for Luc assay and determination of protein concentration. Protein concentration was measured using the Bio-Rad Protein Assay (BIO-RAD, Hercules, CA, USA).

Luc and SEAP assays: The Luc assay was performed according to the manufacturer's instructions for Promega using the Luciferase Assay System. Luc activity, corrected by the protein content of the cell lysate, was expressed in relative light units (RLU)/mg protein. SEAP activity was measured using Great EscAPe™ SEAP Chemiluminescence Kit 2.0 (Clontech, Palo Alto, CA, USA). The luminescence obtained from reactions of the Luc and SEAP assays was then monitored by Glomax™ 96 Microplate Luminometer (Promega).

Quantitative Analysis of CYP1A mRNA contents: Total RNA was extracted using TRI REAGENT® (Molecular Research Center, Cincinnati, OH, USA). First-strand cDNA was synthesized from 1 μg total RNA in a 20 μL reaction mixture using Molony Murein Virus Reverse Transcriptase (Promega), oligo$(dT)_{20}$ primer, and Ribonuclease Inhibitor (TaKaRa Bio). cDNA was used to carry out real-time polymerase chain reaction (PCR) using SYBR Premix ExTaq (TaKaRa Bio) to measure mRNA levels of CYP1A1, CYP1A2, and glyceraldehyde-3-phosphate dehydrogenase (GAPDH). The amplification reaction were performed with specific primers for CYP1A1 (forward: 5′-ACTGCTTAGCCTAGTCAACCTG-3′ and reverse: 5′-CAATCAGGCTGTCTGTGATGTC-3′), CYP1A2 (forward: 5′-CATTGGTGCCATGTGCTTC-GGACAG-3′ and reverse: 5′-AAGTCCTGATAGTGCTC-CTGGACTG-3′), and GAPDH (forward: 5′-GAAGGTG-AAGGTCGGAGTCAAC-3′ and reverse: 5′-CAGAGTTA-AAAGCAGCCCTGGT-3′). Quantitative values were obtained above the threshold PCR cycle number (Ct) at which increase in signal associated with an exponential growth for PCR products was detected using Thermal Cycler Dice™ TP800 (TaKaRa Bio). Relative mRNA expression levels in each sample were normalized according to GAPDH expression levels.

Results

Induction of reporter activities derived from dual reporter genes of *CYP1A1* and *CYP1A2* by TCDD in the stable cell line: The stable cell line that constitutively expressed reporter activities was constructed by inserting the dual reporter plasmid containing the 23-kb intergenic spacer region, responsible for transcriptional activation and regulation of *CYP1A1* and *CYP1A2* genes into the chromosome of HepG2 cells. The transcriptional activities of *CYP1A1* and *CYP1A2* genes were measured simultaneously with Luc and SEAP activities, respectively. To characterize the isolated stable cell line, a time-course and dose-dependent induction of reporter activities by TCDD was measured. The reporter activities were determined at 3 time intervals (24, 48, and 72 h) after adding the concentrations ranging from 0.001 to 100 nM of TCDD to the culture medium. TCDD response of Luc and SEAP in the stable cell line increased in a time-course and dose-dependent manner (**Fig. 1**). Maximum induction occurred when cells were exposed to 10 nM for 72 h, during which Luc and SEAP activities were observed at 200- and 30-fold inductions, respectively. In addition, the reporter activities were readily detectable in the stable cell line, even though a low concentration of TCDD (1 nM) for 48 h was used.

The effects of various cell densities on Luc and SEAP activities were also examined. The stable cell line was seeded at densities of 2.5×10^4, 5×10^4, and 10×10^4 cells, and reporter activities were determined after 48 h treatment with 1 nM and 10 nM TCDD, respectively. As expected, enhancement of the reporter activities occurred in a cell density-dependent manner with the 10×10^4 cell density exhibiting the greatest elevation (**Fig. 2**).

Influence of inducer concentration and exposure period on reporter activity: TCDD has a long half-life (5–11 years in humans) owing to its high lipophilicity and little or no metabolism.[16–20] Therefore, in this system, TCDD accumulated in the stable cell line. On the other hand, a number of CYP1A1/1A2 inducers such as PAHs, therapeutic agents, and endogenous compounds are substrates for the enzymes. Among prototypical AhR ligands, 3-MC and IND are rapidly metabolized by drug metabolism enzymes and lose their ligand activity.[21,22] To confirm time- and dose-dependent change of Luc activity, the stable cell line was treated with TCDD, 3-MC, and IND under the same conditions (**Fig. 3**). The inducible potency of 3-MC and IND decreased from 24 to 72 h, whereas TCDD caused induction that remained maximal for the entire 72 h duration of the experiment.

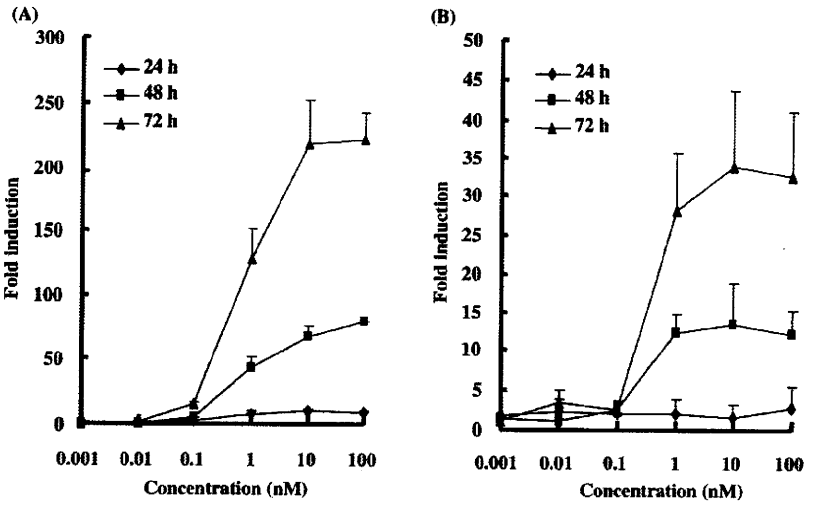

Fig. 1. Time-course and dose-dependent induction of reporter activities by TCDD in the stable cell line
Cells were seeded at 5.0×10^4 cells in 24-well tissue culture plates and treated with TCDD (0.001–100 nM). Cells were harvested at 24 (closed diamonds), 48 (closed squares), and 72 h (closed triangles) after TCDD treatment, and the lysate was used for assays of Luc activity and protein concentration. The assay of SEAP activity used a portion of the media. Luc and SEAP activities were normalized with protein concentration, and the values are each shown as the ratio of the average for the control treated with 0.1% DMSO. Each paint represents the means of 3 samples and the error bars represent standard deviations. (A) Luc activity, (B) SEAP activity.

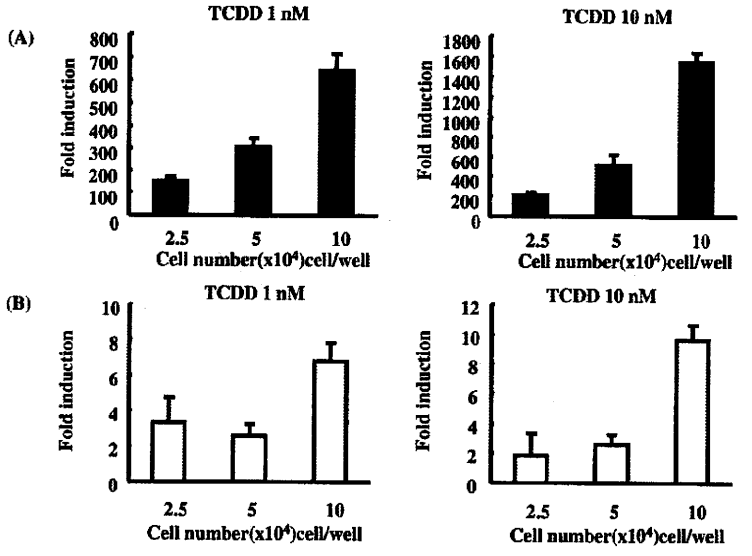

Fig. 2. The effects of various cell densities on reporter activities induced by TCDD in the stable cell line
Cells were seeded in 24-well tissue culture plates at the densities of 2.5×10^4, 5×10^4, and 10×10^4 cells/well 24 h before TCDD treatment. Cells were treated for 48 h and the lysate was harvested. The lysate was used for assays of Luc activity and protein concentration. The assay of SEAP activity used a portion of the media. Luc and SEAP activities were normalized with protein concentration, and the values are each shown as the ratio of the average for the control treated with 0.1% DMSO. The columns represent the means of 3 samples and error bars represent standard deviations. (A) Luc activity, (B) SEAP activity.

Because the stable cell line was treated with low concentrations of CYP1A1/1A2 inducers, induction via measurement of SEAP activity was not determined.

Induction of reporter activities compared between the stable cell line and transient expression system: The reporter activities of the stable cell line were significantly enhanced in response to TCDD. To assess the sensitivity of CYP1A1/1A2 induction screening, the fold induction of reporter activities in the stable cell line was compared with that in the transient expres-

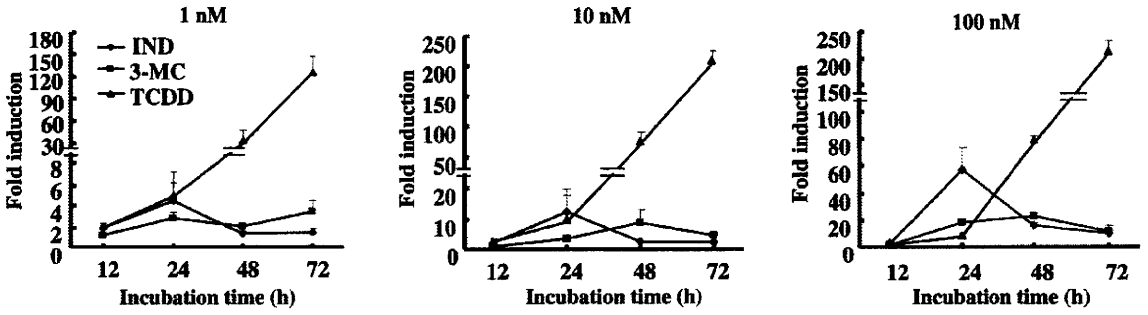

Fig. 3. Time- and dose-dependent changes of Luc activity induced by AhR ligands in the stable cell line
Cells were seeded at 5.0×10^4 cells in 24-well tissue culture plates and treated with IND (closed diamonds), 3-MC (closed squares), and TCDD (closed triangles) (1–100 nM). Cells were harvested at 12, 24, 48, and 72 h after compound treatment and the lysate was used for assays of Luc activity and protein concentration. Luc activity was normalized with protein concentration, and the values are each shown as the ratios of the average for the control treated with 0.1% DMSO. Each paint represents the means of 3 samples and error bars represent standard deviations.

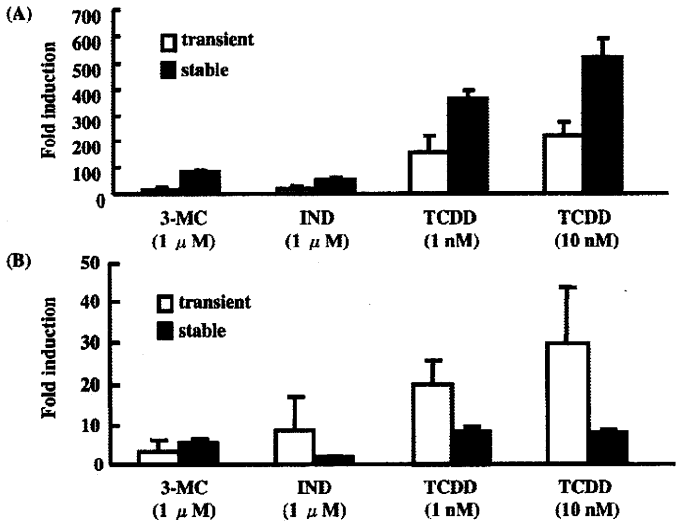

Fig. 4. Comparison of induction response for typical CYP1A1/1A2 inducers between the stable cell line and transient expression system
Cells were seeded 1.0×10^5 cells/well in 24-well tissue culture plates with 0.5 mL of DMEM for 24 h before compound treatment. HepG2 cells were seeded 1.0×10^5 cells/well in 24-well tissue culture plates with 0.5 mL of DMEM for 20 h before transfection. The pd-1A1/1A2 dual reporter gene plasmid (0.8 μg) was transiently transfected using Targefect F-1 according to the manufacturer's instructions and incubated for 4 h. Two cells (stable cell line; closed bars, transient expression system; open bars) were treated with TCDD (1 nM and 10 nM), 3-MC (1 μM), and IND (1 μM) for 48 h. Then, reporter activities were measured. Luc and SEAP activities were normalized by protein concentration, and the values are each shown as the ratio of the average for the control treated with 0.1% DMSO. The columns represent the means of 3 samples and the error bars represent standard deviations. (A) Luc activity, (B) SEAP activity.

sion system using HepG2 and pd-1A1/1A2 (**Fig. 4**). Two CYP1A1/1A2 induction screening systems were exposed to 3 strong inducers of CYP1A1/1A2: TCDD, 3-MC, and IND. As a result, the responsiveness of Luc activity in the stable cell line was observed as both more sensitive and more stable than that of the transient expression system (**Fig. 4A**). The Luc activity of the stable cell line was elevated 2-fold compared to the transient expression system. In contrast, the induction of SEAP activity in the stable cell line was less than that in the transient expression system (**Fig. 4B**). However, when the 2 experiments were treated with 3-MC, the responsiveness of SEAP activity in the stable cell line was equivalent to that in the transient expression system. These results show that the stable cell line is an adequately sensitive assay for assessing typical CYP1A1/1A2 inducers.

Transcriptional activation of *CYP1A1* and *CYP1A2* genes by various compounds: To demonstrate the utility of the stable cell line for typical CYP1A1/1A2 inducers, cells were treated with proton

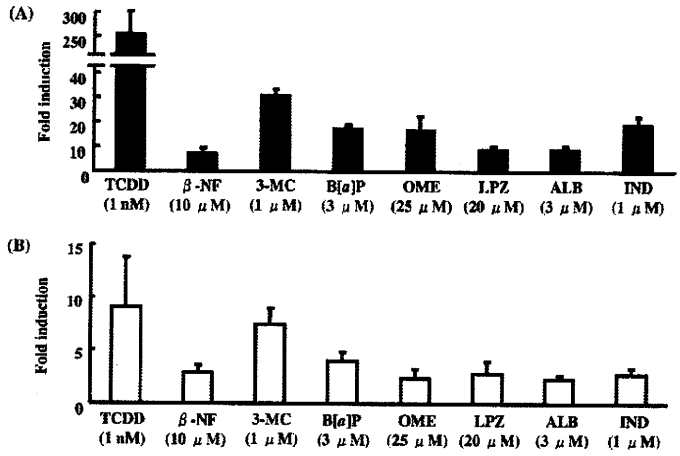

Fig. 5. Transcriptional activation of *CYP1A1* and *CYP1A2* genes by various CYP1A1/1A2 inducers in the stable cell line
Cells were seeded 1.0×10^5 cells/well in 24-well tissue culture plates with 0.5 mL of DMEM 24 h before treatment with various compounds. The cells were treated with TCDD (1 nM), β-NF (10 μM), 3-MC (1 μM), B[*a*]P (3 μM), OME (25 μM), LPZ (20 μM), ALB (3 μM), and IND (1 μM) for 48 h. Then, reporter activities were measured. Luc and SEAP activities were normalized by protein concentration, and the values are each shown as the ratio of the average for the control treated with 0.1% DMSO. The columns represent the means of 3 samples and the error bars represent standard deviations. (A) Luc activity, (B) SEAP activity.

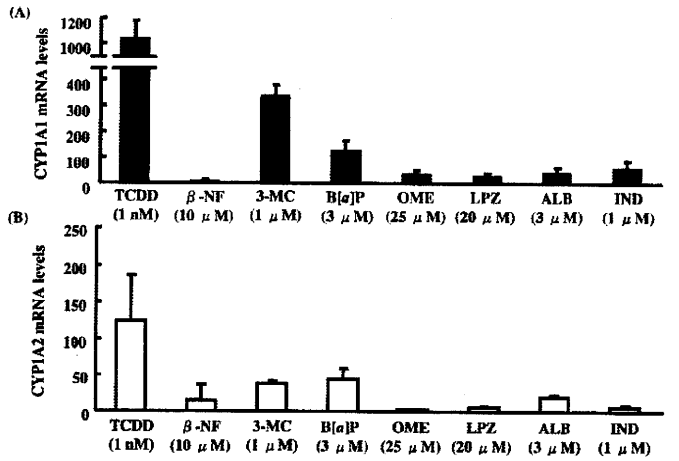

Fig. 6. Influence of various CYP1A1/1A2 inducers on CYP1A1 and CYP1A2 mRNA levels in the stable cell line.
Cells were seeded 2.0×10^5 cells/well in 12-well tissue culture plates with 1 mL of DMEM for 24 h before compound treatment. The cells were treated with TCDD (1 nM), β-NF (10 μM), 3-MC (1 μM), B[*a*]P (3 μM), OME (25 μM), LPZ (20 μM), ALB (3 μM), and IND (1 μM) for 48 h. After 48 h, total mRNA was extracted and subjected to quantitative reverse-transcriptase PCR. GAPDH was used as the internal standard. Each value is shown as the ratio of the average for the control treated with 0.1% DMSO. The columns represent the means of 3 samples and the error bars represent standard deviations. (A) CYP1A1 mRNA level, (B) CYP1A2 mRNA level.

pump inhibitors, ALB, IND, PAHs, and TCDD (**Fig. 5A** and **B**).[23-27] Among these compounds, TCDD (1 nM) produced the maximum increase in Luc activity, which was 263.6 ± 49.9-fold above DMSO-treated cells (**Fig. 5A**). Among the PAHs tested, 3-MC (1 μM) and B[*a*]P (3 μM) were also strong CYP1A1 inducers; they increased the Luc activity by 31.1 ± 2.2-fold and 17.7 ± 1.3-fold, respectively. When cells were treated with therapeutic agents such as proton pump inhibitors (OME 25 μM and LPZ 20 μM) and ALB (3 μM), Luc activity was elevated from 9.0 ± 1.0-fold to 17.1 ± 5.2-fold compared to that with DMSO control. IND (1 μM), an endogenous ligand for AhR isolated from normal human urine, also increased Luc activity (19.5 ± 2.9-fold). As with Luc activity, SEAP activity was also elevated 9.1 ± 4.7-fold upon TCDD treatment. Furthermore, 3-MC and B[*a*]P produced 7.4 ± 1.5-fold and 3.9 ± 0.9-fold increases in SEAP activity, respectively (**Fig. 5B**). Although induction of simultaneously measured SEAP activity was lower than that of Luc activity, the induction pattern among the test-

ed compounds was similar between the Luc and SEAP activities.

As shown in **Figures 6A** and **B**, intrinsic CYP1A1 and CYP1A2 mRNA levels substantially increased in the stable cell line treated with the various compounds described above. The profile of enhanced CYP1A1 and CYP1A2 mRNA levels was similar to that of the reporter gene assay (**Fig. 6A**). The level of CYP1A1 mRNA induced by TCDD was more than 1,000-fold above the DMSO-treated cells. 3-MC, B[*a*]P, proton pump inhibitors, ALB, and IND produced significant increases in CYP1A1 mRNA level that were more than 30-fold above the DMSO control, while β-NF moderately enhanced mRNA level compared to other compounds. The influence of various compounds on CYP1A2 mRNA level was also examined (**Fig. 6B**). Similar to the results observed with the reporter gene assay, TCDD produced the maximum increase of 124.6 ± 61.6-fold above the

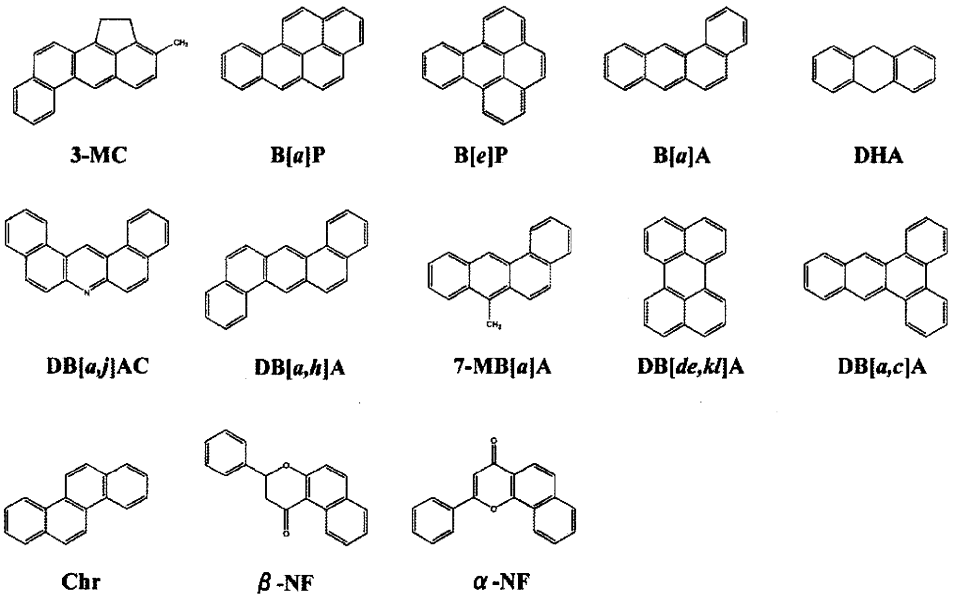

Fig. 7. Structures of PAHs used in this study

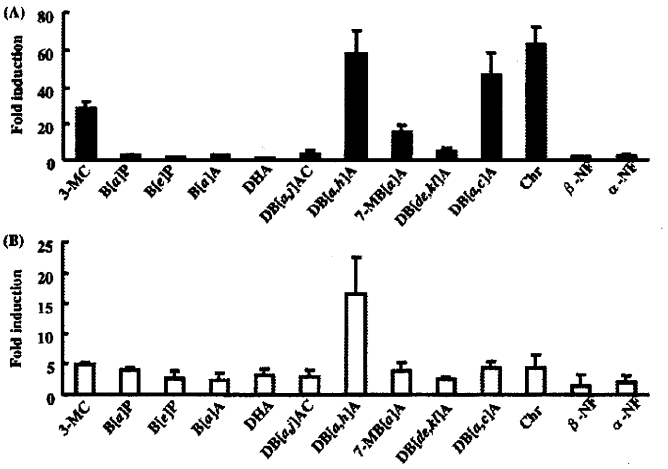

Fig. 8. Screening for assessment of CYP1A1/1A2 induction by 13 PAHs
Cells were seeded 1.0×10^5 cells/well in 24-well tissue culture plates with 0.5 mL of DMEM for 24 h before treatment with the various compounds. The cells were treated with 1 μM of 3-MC, B[*a*]P, B[*e*]P, B[*a*]A, DHA, DB[*a,j*]AC, DB[*a,h*]A, 7-MB[*a*]A, DB[*de,kl*]A, DB[*a,c*]A, Chr, β-NF, α-NF for 48 h. Then, reporter activities were measured. Luc and SEAP activities were normalized by protein concentration, and each value is shown as the ratio of the average for the control treated with 0.1% DMSO. The columns represent the means of 3 samples and the error bars represent standard deviations. (A) Luc activity, (B) SEAP activity.

DMSO control in CYP1A2 mRNA levels. 3-MC and B[*a*]P also proved to be strong inducers for CYP1A2 mRNA, resulting in 37.8 ± 4.5-fold and 44.2 ± 14.9-fold increases, respectively. These experiments demonstrate that induction profiles of the reporter activities in a stable cell line treated with typical CYP1A1/1A2 inducers are closely correlated to those that increase intrinsic CYP1A1 and CYP1A2 mRNA levels.

Screening assays for assessing transcriptional activation of *CYP1A1* and *CYP1A2* genes by PAHs: The extent of CYP1A1/1A2 induction activity differs for each PAH, although both are highly induced by PAHs. In order to further substantiate the ability of the stable cell line to be used to assess CYP1A1/1A2 inducers, cells were treated with 13 PAHs (1 μM, **Fig. 7**). As shown in **Figures 8A** and **B**, DB[*a,h*]A produced significant increases in Luc and SEAP activities that were 58.0 ± 12.1-fold and 16.6 ± 6.0-fold above the DMSO control, respectively. On the other hand, DB[*a,c*]A and Chr appeared to be strong inducers of Luc activity only, resulting in increases that were 46.5 ± 11.6-fold and 63.0 ± 9.3-fold above the DMSO control, respectively (**Fig. 8A**). Furthermore, Luc activity was also enhanced by 3-MC and 7-MB[*a*]A. The remaining PAHs did not induce Luc activity greater than 5-fold compared to the DMSO control. SEAP activity of the stable cell line treated with all tested PAHs (except for DB[*a,h*]A) exhibited modest induction and similar extents (**Fig. 8B**). These results show that the stable cell line has high reporter activities at relatively low concentration (1 μM) that were easily detectable on CYP1A1/1A2 induction.

Discussion

CYP1A1/1A2 induction has significant implications in the pharmacokinetics and toxicity of xenobiotics such as therapeutic agents and environmental chemicals. To date, information about CYP1A1/1A2 induction has been obtained via measurement of specific enzyme activity and mRNA expression level in cellular systems such as human hepatocytes and human hepatoma cell lines.[28-31] The most relevant information was derived from enzyme activity in human hepatocytes. However, methods for determining enzyme activity are time consuming and require cumbersome laboratory procedures and are therefore low-throughput. On the other hand, the reporter gene assay is well suited for high-throughput screening to assess induction of CYP1A1/1A2.[32]

To test the stable cell line created in this study, induction of reporter activities by strong CYP1A1/1A2 inducers was measured. TCDD induced activity in a time-, dose-, and cell density-dependent manner (**Figs. 1** and **2**). When the stable cell line was treated with 1 nM TCDD for 48 h, enhancement of both Luc (642.3 ± 72.5-fold) and SEAP (6.8 ± 1.0-fold) activities was significant enough to simultaneously assess the transcriptional activation of *CYP1A1* and *CYP1A2* genes under optimal conditions. Other researchers have established similar reporter cell lines—101L cells and DRE12–6 cells—for assessing CYP1A1 induction.[33] In 101L cells, 2 nM TCDD produced a 22-fold increase in Luc activity after 24 h of exposure.[34] DRE12–6 cells treated for 28 h with 10 nM TCDD exhibited a 20-fold increase in Luc activity.[10] However, 101L and DRE12–6 cells integrated only part of the *CYP1A1* promoter region and 3 copies of XRE, respectively. In addition, these reporter gene systems were not capable of assessing CYP1A2 induction. Although it is difficult to directly compare the results obtained under various conditions, the stable cell line generated in this study exhibited high sensitivity to TCDD in CYP1A1/1A2 induction.

To demonstrate the utility of the stable cell line for the majority of compounds previously identified as CYP1A1/1A2 inducers, cells were treated with proton pump inhibitors, ALB, IND, PAHs, and TCDD (**Figs. 5A** and **B**). The results clearly show that all compounds caused induction of reporter activity. The fold induction in the SEAP activity was lower than that of the Luc activity, while the induction pattern among tested compounds resulted in similar induction of Luc and SEAP activities. In addition to assessing transcriptional activation of *CYP1A1* and *CYP1A2* genes by measuring reporter activities, we determined that the same compounds altered intrinsic CYP1A1 and CYP1A2 mRNA levels (**Figs. 6A** and **B**). In general, most compounds exhibiting induction in the reporter assay also exhibited increased CYP1A1 and CYP1A2 mRNA levels. Other researchers have demonstrated pharmacologic profiling of CYP1A1/1A2 induction in HepG2 cells and human hepatocytes.[35] Use of mRNA expression to detect CYP1A1/1A2 induction helps predict the enhancement of these enzymatic activities and increases the throughput. In the present study, detection of CYP1A1 and CYP1A2 mRNA levels was more sensitive than the reporter activities derived from a dual reporter gene. One reason for this is that the reporter gene assays generally display high backgrounds. However, the reporter gene assays have the advantages of being readily available and reproducible, and they are well suited for high-throughput screening approaches. The stable cell line created in this study indicated a similar effect in the induction response of reporter activities and intrinsic CYP1A1 and CYP1A2 mRNA levels. Accordingly, the enhancement of reporter activities in the stable cell line sufficiently reflected responses of *in vivo* CYP1A1/1A2 induction at a level comparable to that of specific enzyme activity and mRNA expression level in human hepatocytes and human hepatoma cell lines.

In order to further substantiate the ability of the stable cell line to assess CYP1A1/1A2 inducers, 13 PAHs were used to treat the cells (**Figs. 8A** and **B**). The induction profile of the SEAP activity by PAHs was similar to that of